DOI: 10.1002/cmdc.201000514

Design, Synthesis, and Pharmacological Characterization of Novel Spirocyclic Quinuclidinyl-Δ^2-Isoxazoline Derivatives as Potent and Selective Agonists of α7 Nicotinic Acetylcholine Receptors

Clelia Dallanoce,[a] Pietro Magrone,[a] Carlo Matera,[a] Fabio Frigerio,[a] Giovanni Grazioso,[a] Marco De Amici,[a] Sergio Fucile,[b, c] Vanessa Piccari,[b] Karla Frydenvang,[d] Luca Pucci,[e] Cecilia Gotti,[e] Francesco Clementi,[e] and Carlo De Micheli*[a]

A set of racemic spirocyclic quinuclidinyl-Δ^2-isoxazoline derivatives was synthesized using a 1,3-dipolar cycloaddition-based approach. Target compounds were assayed for binding affinity toward rat neuronal homomeric (α7) and heteromeric (α4β2) nicotinic acetylcholine receptors. Δ^2-Isoxazolines **3a** (3-Br), **6a** (3-OMe), **5a** (3-Ph), **8a** (3-O*n*Pr), and **4a** (3-Me) were the ligands with the highest affinity for the α7 subtype (K_i values equal to 13.5, 14.2, 25.0, 71.6, and 96.2 nM, respectively), and showed excellent α7 versus α4β2 subtype selectivity. These compounds, tested in electrophysiological experiments against human α7 and α4β2 receptors stably expressed in cell lines, behaved as partial α7 agonists with varying levels of potency. The two enantiomers of ($\pm$)-3-methoxy-1-oxa-2,7-diaza-7,10-ethanospiro[4.5]dec-2-ene sesquifumarate **6a** were prepared using (+)-dibenzoyl-L- or (−)-dibenzoyl-D-tartaric acid as resolving agents. Enantiomer (*R*)-(−)-**6a** was found to be the eutomer, with K_i values of 4.6 and 48.7 nM against rat and human α7 receptors, respectively.

Introduction

Nicotinic acetylcholine receptors (nAChRs) are members of the Cys-loop superfamily of ligand-gated ion channels, which, in mammals, also encompasses the serotonin 5-HT_3, γ-aminobutyric acid ($GABA_A$ and $GABA_C$), and glycine receptors.[1] The nAChRs, which are involved in physiological responses to the neurotransmitter acetylcholine (ACh), are extensively distributed throughout the peripheral and central nervous system (CNS).[2] These receptors are assemblies of five distinct transmembrane proteins (subunits), each characterized by a large extracellular N-terminal domain, four membrane-spanning alpha helices, and a short C-terminal domain.[3] Neuronal nAChRs are localized on the postsynaptic neuronal terminals or act as presynaptic receptors, thus indirectly modulating the release of various key neurotransmitters including dopamine, serotonin, GABA, glutamate, histamine, and norepinephrine.[4] The nAChR subunits are encoded by seventeen genes, and twelve subunits have been identified to date in the brain: nine α (α2–α10) and three β (β2–β4) subunits, which assemble to form either homopentamers (α7 or α9) or heteropentamers (α9/α10 and α/β).[5] However, a relatively small subset of α/β combinations generates functionally and physiologically relevant channels. It has been postulated that α homomeric receptors have five identical ACh binding sites per receptor complex, each located at the subunit interface, while heteromeric receptors have binding sites located solely at the interface between an α and a β subunit.[6] The subunit composition of neuronal nAChRs affects both their response to exogenous ligands and their permeability to cations (Na^+, K^+ and Ca^{2+}). In general, receptors characterized by heteromeric combinations of α4 and β2 subunits, with putative $(\alpha4)_2(\beta2)_3$ stoichiometry, show high affinity for the agonist (*S*)-nicotine. Conversely, homopentameric receptors, that is, the α7 subtype, strongly bind antagonists such as α-bungarotoxin and methyllycaconitine. In terms of intrinsic Ca^{2+} permeability, neuronal heteromeric α/β nAChRs have a fractional Ca^{2+} current of 2–5%,[7] which increases to 6–12% for homomeric α7 receptors.[7]

[a] *Dr. C. Dallanoce, Dr. P. Magrone, Dr. C. Matera, Dr. F. Frigerio, Dr. G. Grazioso, Prof. M. De Amici, Prof. C. De Micheli*
Dipartimento di Scienze Farmaceutiche Pietro Pratesi
Università degli Studi di Milano
Via Mangiagalli 25, 20133 Milan (Italy)
Fax: (+39) 02-50319326
E-mail: carlo.demicheli@unimi.it

[b] *Prof. S. Fucile, Dr. V. Piccari*
Dipartimento di Fisiologia e Farmacologia
Università di Roma La Sapienza
Piazzale A. Moro 5, 00185 Rome (Italy)

[c] *Prof. S. Fucile*
Istituto Neurologico Mediterraneo Neuromed
Via Atinese 18, 86077 Pozzilli (Italy)

[d] *Prof. K. Frydenvang*
Department of Medicinal Chemistry
The Faculty of Pharmaceutical Sciences, University of Copenhagen
Universitetsparken 2, 2100 Copenhagen (Denmark)

[e] *Dr. L. Pucci, Dr. C. Gotti, Prof. F. Clementi*
CNR, Istituto di Neuroscienze, Farmacologia Cellulare e Molecolare
Dipartimento Farmacologia, Chemioterapia e Tossicologia Medica
Università degli Studi di Milano
Via Vanvitelli 32, 20129 Milan (Italy)

The heteromeric α4β2 subtype is, by far, the most widely distributed nAChR in the CNS, while among the homomeric receptor population in the brain, expression of the α7 subtype is highest. The two subtypes are differently localized throughout the CNS; however, they are coexpressed in the hippocampus and the cortex,[4] which play a major role in cognitive processes such as learning and memory consolidation. Ligands acting at these two nAChR subtypes could be promising drug candidates for therapeutic intervention in a range of pathologies, including Alzheimer's and Parkinson's diseases, epilepsy, schizophrenia, Tourette's syndrome, attention deficit hyperactivity disorder, pain, depression, and tobacco addiction.[2,8] Initially, α4β2 nAChRs were the privileged molecular target of analogues of natural compounds such as nicotine, epibatidine, and cytisine that were designed by pharma companies and academia with the aim of discovering selective agonists for development as drug candidates to treat a number of neurodegenerative diseases.[9] Recently, a growing number of reports has focused on derivatives designed as selective α7 nAChR ligands.[3b,10] The interest in α7 selective agonists/partial agonists is mainly related to deficits in auditory sensory processing, which lead to a state of sensory overload and contribute to the attentional and cognitive dysfunctions that are the hallmark of various CNS diseases such as schizophrenia.[11] Moreover, the administration of α7 selective agonists, either alone or in association with antipsychotic drugs, exhibited in vivo efficacy in preclinical models predictive of cognitive-enhancing and antipsychotic-like activities.[12] Furthermore, there is growing evidence that ligands selectively targeting α7 nAChRs may modulate cellular functions beyond synaptic transmission, making them potentially useful drugs for innovative therapeutic indications other than CNS pathologies. As the presence of α7 nAChRs in peripheral cholinergic pathways has been demonstrated,[13] selective agonists of this subtype are emerging as promising drug candidates for the treatment of inflammation and pain.[14] Finally, a rapidly progressing research line is the allosteric modulation of nAChRs, primarily focused on positive modulators of the α7 subtype, that is, compounds which lack intrinsic efficacy for direct stimulation of the receptor but enhance agonist-induced receptor activation.[8c,15]

The rigid quinuclidine scaffold or similar bicyclic tertiary bases represent first choice core fragments for molecular recognition of ligands by the α7 channel protein.[16] Structures of some of the most promising full/partial α7 agonists have been collected and are shown in Figure 1, including the quinuclidine ligands AR-R17779,[10a,17] PNU-282987,[18] JN403,[19] and TC-5619,[12b] and azabicyclic or diazabicyclic compounds SSR180711[20] and PHA-709829.[21]

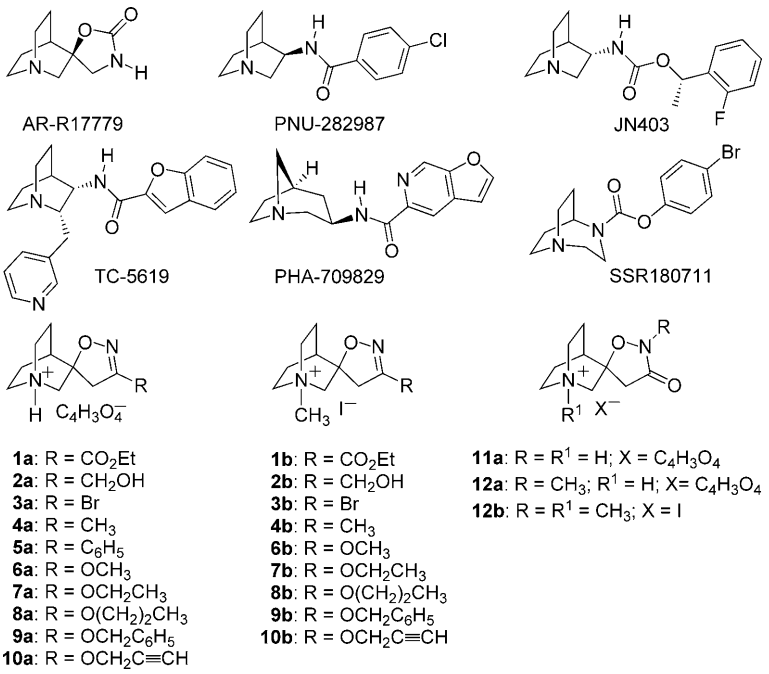

Figure 1. Structures of selected reference α7 nAChR agonists/partial agonists and of the spirocyclic quinuclidinyl derivatives investigated in this study.

As part of an ongoing research program devoted to the study of novel heterocyclic derivatives targeting neuronal nAChRs,[22] we report herein the results obtained for a selected group of nicotinic ligands which have been described in a patent application.[22d] This paper deals with the synthesis of a set of spirocyclic quinuclidinyl-Δ^2-isoxazolines (**1a**–**10a**) and two quinuclidinyl-isoxazolin-3-ones (**11a** and **12a**) whose structure is reported in Figure 1. The corresponding quaternary methyl iodides **1b**–**4b**, **6b**–**10b**, and **12b** (Figure 1), ligands potentially acting at peripheral nAChRs, were also prepared and tested.

The target compounds were initially evaluated for their binding affinity toward the α7 and α4β2 nAChR subtypes, followed by a study of the electrophysiological profile of the most relevant ligands. Furthermore, the two enantiomers of the most promising α7 selective agonist, **6a**, were prepared and tested. The (*R*)-configuration was attributed to the eutomer by X-ray structural analysis, and its binding mode was investigated by molecular docking in a model of the α7 nAChR subtype.

Results and Discussion

Our approach to target compounds is based on the versatile 1,3-dipolar cycloaddition of nitrile oxides to suitable dipolarophiles to yield Δ^2-isoxazoline derivatives. We have used this strategy extensively over the last decade to synthesize a large number of biologically active compounds.[23] In the present

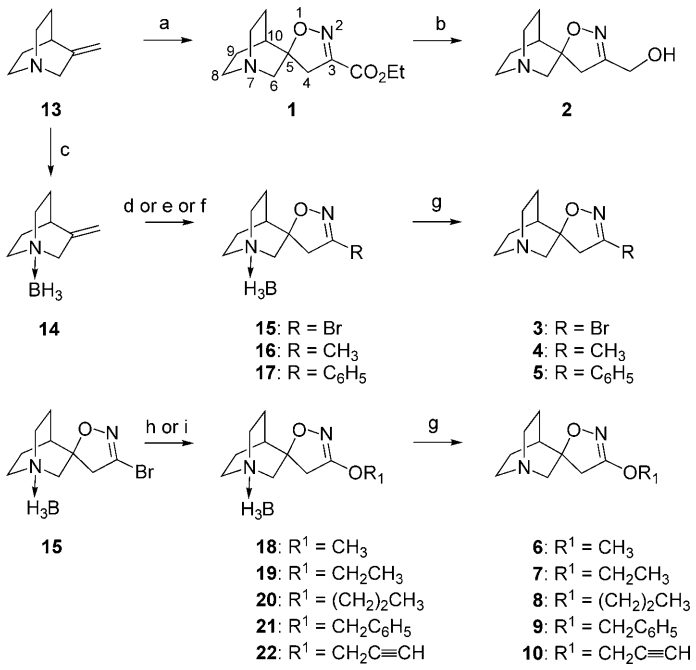

Scheme 1. *Reagents and conditions*: a) $Et_2OCC(Cl)=NOH$ (4 equiv), $NaHCO_3$, dioxane, reflux, 4 d, 13%; b) $NaBH_4$, EtOH, RT, 5 h, 48%; c) 1.0 M BH_3·THF complex, 0 °C→RT, 30 min, 84%; d) $Br_2C=NOH$ (3 equiv), K_2CO_3, EtOAc, RT, 5 d, 48%; e) $CH_3C(Cl)=NOH$ (9 equiv), Et_3N, CH_2Cl_2, RT, 48 h, 30%; f) $C_6H_5CH=NOH$ (5 equiv), $NaOCl_{(aq)}$, CH_2Cl_2, RT, 5 d, 16%; g) CF_3CO_2H, acetone, RT, 12 h, 70%; h) MeOH (or EtOH), K_2CO_3, RT, 16 h, 81%; i) NaH, THF, *n*PrOH (or $C_6H_5CH_2OH$ or $HC\equiv CCH_2OH$), 0 °C→RT, 16 h, 74%.

study, the racemic spirocylic Δ^2-isoxazolines and isoxazolidin-3-ones were synthesized by reacting 3-methylene-1-azabicyclo-[2.2.2]octane **13**, or its borane complex **14**, with various nitrile oxides under a variety of experimental conditions (Scheme 1). Initially, olefin **13**,[24] in dioxane at reflux, was combined with excess ethoxycarbonylformonitrile oxide, generated in situ with sodium bicarbonate from its stable precursor, ethyl 2-chloro-2-(hydroximino)-acetate.[25] This pericyclic process gave the expected ester **1** in very low yield (13%); the cycloadduct was converted into the related primary alcohol **2** by treatment with sodium borohydride.

In order to improve the yield, dipolarophile **13** was transformed into the more reactive *N*-boranyl alkene **14**[26] using a 1.0 M solution of borane–THF complex (BH_3·THF). As expected, reaction of **14** with bromonitrile oxide[27a] and acetonitrile oxide[27b] afforded spirocyclic cycloadducts **15** and **16** in higher yields (48% and 30%, respectively, Scheme 1). The corresponding 3-phenyl-Δ^2-isoxazoline **17** was obtained in 16% yield following the reaction of **14** with benzonitrile oxide, generated in situ from benzaldoxime and aqueous sodium hypochlorite.[27c] The *N*-boranyl moiety of intermediates **15**, **16**, and **17** was easily removed by treatment with an acetone solution of trifluoroacetic acid, yielding the desired quinuclidinyl free bases **3**, **4**, and **5**, respectively. Notably, compounds **4** and **5** were previously prepared and tested as potential acetylcholinesterase inhibitors.[24]

The intermediate Δ^2-isoxazoline **15** underwent efficient nucleophilic displacement of bromine by various alcohols in basic medium (potassium carbonate or sodium hydride suspension) to produce the corresponding alkoxy *N*-boranyl Δ^2-isoxazolines **18**–**22**, which were readily transformed into final tertiary bases **6**–**10**. As illustrated in Scheme 2, standard catalytic hydrogenation of 3-benzyloxy-Δ^2-isoxazoline **21** produced the cyclic carbamate **23**,[28] which was then transformed into its N-methylated analogue **24** by treatment with iodomethane in an acetone suspension of potassium carbonate. Removal of the boranyl protecting group from **23** and **24** gave free bases **11** and **12** in high yield. Tertiary amines **1**–**12** were treated with fumaric acid to give the related crystalline salts **1a**–**12a**. Alternatively, tertiary amines **1**–**4**, **6**–**10**, and **12** were combined with methyl iodide to afford the corresponding iodomethylates **1b**–**4b**, **6b**–**10b**, and **12b** (Scheme 2).

Target compounds **1a**–**12a**, **3b**, **4b**, and **6b**–**10b** were assessed for binding affinity to α7 and α4β2 rat nAChR subtypes using [^{125}I]α-bungarotoxin and [^{3}H]epibatidine as radioligands, respectively. K_i values, calculated from competition curves using the LIGAND program,[29] are presented in Table 1, with values from α7 nAChR agonists in Figure 1 that were used as reference compounds. These data show that the simultaneous presence of the quinuclidinyl and Δ^2-isoxazolinyl moieties, coupled with the stereoelectronic features of the substituent at position 3 of the spirocyclic system, are crucial structural requirements for productive molecular recognition by the homomeric α7 receptor subtype. Indeed, in the series of fumarates, Δ^2-isoxazolines **3a** (3-Br), **6a** (3-OCH_3), **5a** (3-C_6H_5), **8a** (3-O*n*Pr), and **4a** (3-CH_3) emerged as the ligands exhibiting the highest affinity for the α7 subtype (K_i values equal to 13.5, 14.2, 25.0, 71.6, and 96.2 nM, respectively). In addition, at heteromeric α4β2 nAChRs, the same set of compounds displayed K_i values ranging from 0.64 μM (**3a**) to 140 μM (**7a**).

As shown, the above cited derivatives (**3a**, **6a**, **5a**, **8a**, and **4a**) possess remarkable α7 vs. α4β2 selectivity (47-, 554-, 880-, 922-, and 95-fold, respectively). A comparison of the data for iodomethylates **1b**–**4b**, **6b**–**10b**, and **12b** with data for their corresponding fumarates demonstrated a general decrease in binding affinity at both nAChR subtypes. Of these, 3-methoxy derivative **6b** emerged as the most selective ligand (about 1900-fold), due to a six-fold reduction in affinity at the α7 subtype (K_i = 91.4 nM), combined with a substantial inability to bind the α4β2 receptor (K_i = 175.4 μM).

Based on the previously discussed binding and selectivity data, we wanted to fully characterize the cholinergic profile of the most promising derivative in the series, the 3-methoxy-Δ^2-isoxazoline **6a**. To this end, we tested **6a** with two additional nAChRs, the human α3β4 subtype, expressed in SH-SY5Y cells, and the human α1β1γδ receptor, expressed in TE671 cells. In addition, we evaluated the compound against five human cloned muscarinic receptors (mAChRs, M_1–M_5). Derivative **6a** showed marginal binding affinity for both α3β4 (K_i = 15 μM) and α1β1γδ subtypes (K_i = 78 μM), and behaved as a low affinity ligand for muscarinic receptors [K_i values between 1.95 μM

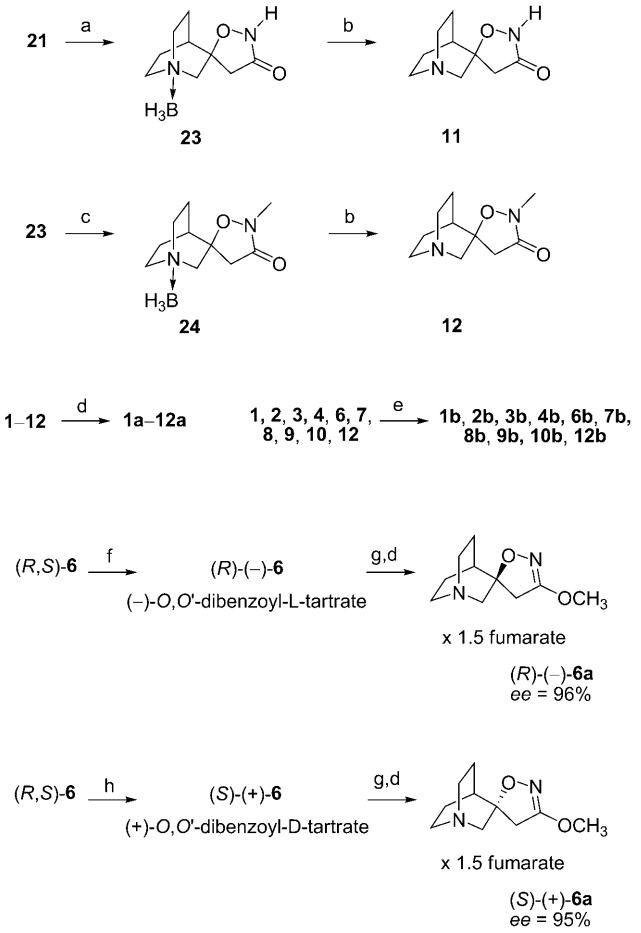

Scheme 2. *Reagents and conditions*: a) H_2, 10% Pd/C, MeOH, 1 atm, 5 h, 97%; b) CF_3CO_2H, acetone, RT, 12 h, 54%; c) CH_3I, K_2CO_3, acetone, RT, 16 h, 88%; d) $C_4H_4O_4$, MeOH, 12 h, 100%; e) CH_3I, MeOH, 12 h, 100%; f) (*R*,*R*)-(−)-*O*,*O*′-dibenzoyl-L-tartaric acid, EtOH (crystallizations from MeOH), 5 d, 18%; g) 20% NaOH, CH_2Cl_2 extraction, 15 min, 100%; h) (*S*,*S*)-(+)-*O*,*O*′-dibenzoyl-D-tartaric acid, EtOH (crystallizations from MeOH), 5 d, 18%.

Table 1. Affinity of derivatives **1a–12a**, **3b**, **4b**, and **6b–10b** for native α4β2 and α7 nAChR subtypes present in rat cortical membranes, labeled by [^{3}H]epibatidine and [^{125}I]α-bungarotoxin.

Compd	K_i[a] [nM], $n=4$		Selectivity
	α7 [^{125}I]α-BgTx	α4β2 [^{3}H]Epibatidine	α7/α4β2
1a	132000 (63)	34000 (14)	0.3
1b	n.t.[b]	n.t.[b]	
2a	1450 (39)	120000 (51)	83
2b	n.t.[b]	n.t.[b]	
3a	13.5 (29)	636 (17)	47
3b	109 (23)	32500 (18)	298
4a	96.2 (29)	9090 (13)	95
4b	756 (27)	203000 (18)	269
5a	25.0 (35)	22000 (22)	880
6a	14.2 (34)	7860 (16) 554	
6b	91.4 (36)	175400 (17)	1919
7a	194 (53)	140000 (64)	721
7b	439 (46)	204000 (61)	465
8a	71.6 (44)	66000 (40)	922
8b	833 (55)	173000 (53)	208
9a	326 (48)	63000 (53)	193
9b	3300 (43)	106000 (53)	32
10a	150 (24)	32100 (15)	214
10b	4250 (35)	148600 (19)	35
11a	5700 (43)	20000 (19)	3.5
12a	250 (55)	2800 (18)	11
12b	n.t.[b]	n.t.[b]	
(±)-Epibatidine	0.71 (17)	0.021[c] (15)	
α-BgTx	0.90[c] (20)	n.d.[d]	
AR-R17779	92[e]	16000[e]	174
PNU-282987	24[f]	14%[g]	
SSR180711	22[h]	>5000[i]	
TC-5619	1[l]	2100[l]	2100

[a] K_i values were derived from four competition binding experiments. Numbers in brackets refer to the percent coefficients of variation. The data on some known alpha 7 agonists have been added for comparison. [b] n.t., not tested. [c] K_d values. [d] n.d., not determined. [e] Reference [17]. [f] Reference [30]. [g] Inhibition at 1 μM.[30] [h] Reference [20]. [i] IC_{50} value for the human nAChR subtype.[20] [l] Reference [12b].

(M_3) and 6.55 μM (M_4)]. As the biological data collected for **6a** appeared very promising, we tackled the preparation of its single enantiomers. Racemic base (±)-**6** was reacted with the commercially available (*R*,*R*)-(−)-*O*,*O*′-dibenzoyl-L- or (*S*,*S*)-(+)-*O*,*O*′-dibenzoyl-D-tartaric acid. Fractional crystallization of the salts allowed us to obtain (*R*)-(−)-**6** and (*S*)-(+)-**6** in high enantiomeric excess (Scheme 2). The absolute configuration of the enantiomers was assigned by single crystal X-ray analysis of the salt between (*R*)-(−)-**6** and (*R*,*R*)-(−)-*O*,*O*′-dibenzoyl-L-tartaric acid. The perspective drawing (ORTEP) of this salt is shown in Figure 2.

Tertiary amines (*R*)-(−)-**6** and (*S*)-(+)-**6** were transformed into sesquifumarates (*R*)-(−)-**6a** and (*S*)-(+)-**6a**, which were assayed for binding affinity against membranes containing rat cortical α7 receptors or α7 receptors obtained from human IMR32 neuroblastoma cells (Table 2). The (*R*)-(−)-**6a** enantiomer was shown to be the eutomer, exhibiting a ten-fold higher binding affinity for rat α7 (K_i = 4.6 nM) than human α7 (K_i = 48.7 nM) receptors. Moreover, the molecular recognition of **6a** was characterized by a higher degree of enantio-discrimination at rat α7, as indicated by the eudismic ratios of 24 and 14 (rat α7 and human α7, respectively; see Table 2). Notably, the spatial arrangement of the substituents around the stereogenic center of (*R*)-**6a** is identical to that of the selective α7 agonist (*S*)-AR-R17779 (Figure 1).

Table 2. Comparison of the binding affinities of (*R*)-(−)-**6a** and (*S*)-(+)-**6a** to membrane-bound α7 receptors in rat and human species.

Compd	K_i[a] [nM] ([^{125}I]α-BgTx)	
	α7 (rat)	α7 (human)
(*R*)-(−)-**6a**	4.6 (35)	48.7 (37)
(*S*)-(+)-**6a**	110 (40)	672 (36)
E.R.[b]	24	14

[a] K_i values, determined for membranes obtained from rat cortex or human IMR32 neuroblastoma cells, were derived from three competition binding experiments. Numbers in brackets refer to the percent coefficients of variation. [b] E.R., eudismic ratio: (*S*)-(+)/(*R*)-(−).

Compound (±)-**6a**, its eutomer (*R*)-(−)-**6a**, and the high affinity α7 nAChR ligands **3a**, **5a**, and **8a** were submitted to

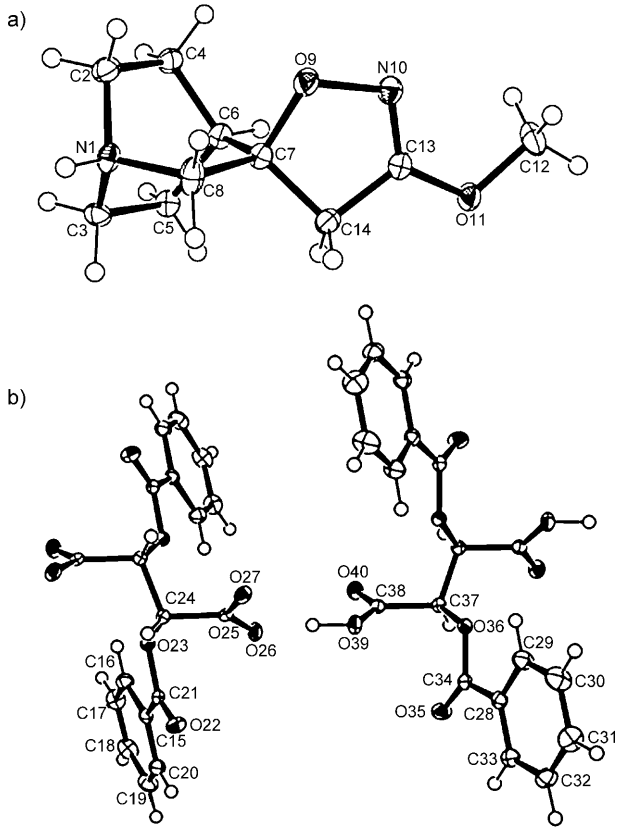

Figure 2. Perspective drawing (ORTEP[41]) of the salt formed by (*R*)-**6** and (*R,R*)-(−)-*O,O′*-dibenzoyl-L-tartaric acid. Displacement ellipsoids of nonhydrogen atoms are shown at the 50% probability level. Hydrogen atoms are represented by spheres of arbitrary size. a) (*R*)-**6**; b) (*R,R*)-*O,O′*-dibenzoyl-L-tartrate.

electrophysiological experiments to assess their functional profiles. The compounds were evaluated against human α7 nAChRs expressed by stable transfection in the rat anterior pituitary GH4C1 cell line,[31a] as well as against human α4β2 and α3β4 nAChRs heterologously expressed in the human HEK 293 cell line.[31b] In addition, we evaluated the ability of **6a** and **3a** to activate or inhibit 5-HT_3 serotonin channels using GH4C1 cells transiently transfected with the human 5-HT_{3A} and 5-HT_{3B} cDNAs. In fact, some α7 selective agonists have been shown to interact at 5HT_3 receptors, behaving as antagonists or partial agonists.[10b] Derivative (±)-**6a** was able to evoke inward whole-cell currents when applied to human α7 GH4C1 cells clamped at −70 mV (Figure 3a). The dose–response relationship indicated an EC_{50} value of 7.7±0.6 μM, with a mean maximal amplitude of 334±21 pA, which was 80±5% of the mean current amplitude elicited by 200 μM ACh ($n=7$, Figure 3d). In contrast, (±)-**6a** evoked negligible currents in human α4β2 HEK cells, with a maximal mean amplitude of 7±2 pA (0.3±0.1% of the ACh-induced response, $n=6$), and in human α3β4-transfected HEK cells (3.3±0.7% of ACh-induced response, $n=9$, data not shown). These data indicate that (±)-**6a** behaves as a partial agonist at α7 nAChRs, exhibiting noteworthy ability to discriminate between the homomeric α7 and the heteromeric nAChR subtypes and thus confirming the binding affinity profile. Next, we tested eutomer (*R*)-(−)-**6a** in the same cell lines, finding similar activation patterns (Figure 3b) with the remarkable difference of a higher response toward human α7 nAChRs when compared to that of 200 μM ACh (177±30%, $n=6$) and an EC_{50} value of 16±9 μM. As (±)-**6a** and eutomer (*R*)-(−)-**6a** induced currents at human α7 nAChRs even in the absence of the exogenously added agonist, it suggests that this nicotinic agonist recognizes the orthosteric site of the α7 receptor, although an additional effect mediated by an allosteric site cannot be ruled out.

High concentrations of (±)-**6a** were able to activate human 5-HT_3 receptors. In fact, inward currents were evoked by (±)-**6a** (EC_{50} >100 μM, Figure 3c) when applied to GH4C1 cells transfected with 5-HT_3 or 5-HT_{3A} and 5-HT_{3B} subunit cDNAs expressing homomeric 5-HT_{3A} and heteromeric 5-HT_{3AB} receptors ($n=6$ and $n=5$, respectively). The maximal current amplitudes mediated by 5-HT_3 receptors activated by 200 μM (±)-**6a** were much smaller (12±5% and 5.7±0.9%) than those evoked by 200 μM serotonin (5-HT) in the same cells, indicating that the compound is a very weak partial agonist of these receptors (Figure 3d).

Similarly to (±)-**6a**, **3a** was able to substantially activate human α7 nAChRs (Figure 4a), with a maximal current amplitude of 542±33 pA elicited by 200 μM **3a** (130±8% of the response induced by 200 μM ACh, $n=6$). However, analysis of the dose–response relationship revealed an EC_{50} value higher than 100 μM, indicating a much lower apparent affinity of **3a** compared to (±)-**6a**. In addition, **3a** showed higher affinity in binding experiments towards both the human α3β4 subtype ($K_i=1.1$ μM) and the human α1β1γδ receptor ($K_i=26$ μM) than **6a**. Also, 3-bromo derivative **3a** emerged as a selective agonist for the α7 nAChRs, being unable to elicit significant inward currents when applied to human α4β2 HEK cells (2.4±0.9% of the response induced by 200 μM ACh, $n=7$, Figure 4b) and human α3β4-transfected HEK cells (1.4±0.9% of ACh-induced response, $n=7$, not shown). Likewise, derivative **3a** weakly activated human 5-HT_{3A} and 5-HT_{3AB} receptors, with maximal current amplitudes representing 2.2±1.5% and 18±6%, respectively ($n=6$, Figure 4c), of the current amplitudes evoked by 200 μM 5-HT in the same cell lines (380±30 and 1700±700 pA, respectively).

The 3-phenyl and 3-*n*-propoxy analogues (**5a** and **8a**, respectively) were also tested for their ability to evoke whole-cell currents mediated by human α7 and α4β2 nAChRs. These derivatives were unable to activate the α4β2 nAChR subtype and acted as weak partial agonists toward α7 nAChRs. Maximal current amplitudes evoked by **5a** and **8a** (200 μM) represented 32±8% and 38±5% of the response induced by 200 μM ACh ($n=6$, data not shown).

In summary, of the compounds evaluated, methoxy derivative **6a** possesses the best structural requirements to act as an agonist, as characterized by high affinity and selectivity for the α7 nAChRs. The substituent at position 3 of the Δ^2-isoxazoline ring affected not only the affinities but also the functional features of derivatives towards the α7 subtype. In fact, gradual increase in the steric bulkiness of the substituent, from bromo (**3a**) and methoxy (**6a**) to phenyl (**5a**) and *n*-propoxy (**8a**),

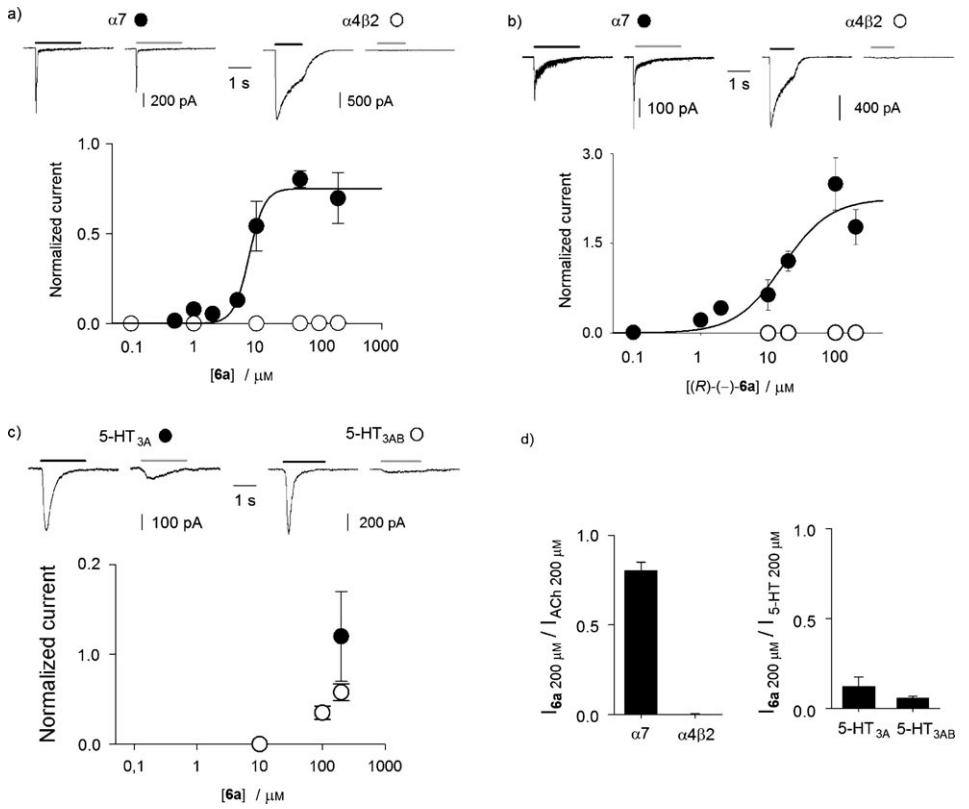

Figure 3. Effects of **6a** on different types of human ligand-gated receptors. a) (top) Typical traces evoked by ACh (black bar, 200 μM) or (±)-**6a** (gray bar, 200 μM) on GH4C1 cells stably transfected with human α7 nAChR subunit (●) or on HEK 293 cells stably transfected with human α4 and β2 nAChR subunits (○), as indicated. Cells were held at −70 mV; (bottom) (±)-**6a** dose-normalized response relationship for human α7 nAChR (●, $n=7$) and for human α4β2 nAChR (○, $n=6$). The Hill equation was best fitted to data obtained from α7 nAChRs, yielding $EC_{50}=7.7\pm0.6$ μM and $n_H=3.5\pm0.7$; b) (top) typical traces evoked by ACh or (*R*)-(−)-**6a** in α7 cells (●, $n=6$) or in α4β2 cells (○, $n=6$), as indicated; (bottom) (*R*)-(−)-**6a** dose-normalized response relationship for human α7 nAChR (●) and for human α4β2 nAChR (○). Hill equation was best fitted to data obtained from α7 nAChRs, yielding $EC_{50}=17\pm10$ μM and $n_H=1.2\pm0.9$; c) (top) typical traces evoked by 200 μM 5-HT or 200 μM (±)-**6a** in GH4C1 cells transiently transfected with the human 5-HT_{3A} subunit (●) or with human 5-HT_{3A} and 5-HT_{3B} subunits (○), as indicated; (bottom) (±)-**6a** dose-normalized response relationship for human 5-HT_{3A} receptors (●, $n=6$) and for human 5-HT_{3AB} receptors (○, $n=6$); d) histograms showing the ratio between the mean current amplitude evoked by 200 μM (±)-**6a** and 200 μM ACh on nicotinic receptors (left, as indicated) or 200 μM 5-HT on 5-HT_3 receptors (right, as indicated).

caused a significant decrease in the α7-mediated electrophysiological response. This result is expected to be even more severe for the remaining O-alkylated analogues **7a**, **9a**, and **10a**, which are characterized by relatively moderate affinities ($K_i=194$, 326, and 150 nM, respectively). The same gradual drop in α7 affinity ($K_i=91.4$, 439, 833, 3300, and 4250 nM, respectively) was observed for the set of O-alkylated methylammonium iodides **6b–10b** which, presumably, is also associated with a stepwise reduced ability to activate the receptors.

The two enantiomers of **6a** were docked into the binding cleft of the human α7 homology model that we recently published,[22b] with the aim of accounting for their differences in affinity. This model has been validated for nicotinic agonists characterized by various structural skeletons.[22b] The binding mode of (*R*)-**6** and (*S*)-**6** was refined by cluster analysis (CA) and molecular mechanics geometry optimization. Similar to other α7 agonists/partial agonists bearing a quinuclidine group, the molecular fragment of (*R*)-**6** efficiently interacted with an aromatic box delimited by the four amino acid residues Trp 54, Trp 148, Tyr 187, and Tyr 194 (Figure 5).

In addition, we detected a hydrogen bond between the protonated nitrogen of the quinuclidine moiety and the side chain of Tyr 92. Moreover, the methoxy group appended to the Δ^2-isoxazoline nucleus of (*R*)-**6** projected into a lipophilic pocket defined by residues Cys 189–Cys 190 (S–S bridge), Leu 119, Leu 108, Val 107, Gln 116, and Tyr 117. An additional hydrogen bond between the 3-methoxy group of (*R*)-**6a** and the side chain of Gln 116 further stabilized the proposed ligand binding mode (Figure 5). The interaction of distomer (*S*)-**6a** with the binding site of the α7 receptor subtype was similar to that displayed by the eutomer. However, due to the opposite orientation of the spirocyclic moiety, the methoxy group of (*S*)-**6a** was unable to form a hydrogen bond with the side chain of Gln 116, which could account for the moderate eudismic ratio found for **6a** at human α7 nAChRs.

Conclusions

In this study, a set of spirocyclic quinuclidinyl-Δ^2-isoxazolines and two quinuclidinyl-isoxazolidin-3-ones were designed and synthesized by exploiting 1,3-dipolar cycloaddition chemistry. Two groups of target compounds—the tertiary bases assayed as fumarates and their corresponding methyl iodides—were prepared and tested for binding affinity at rat α7 and α4β2 nAChR subtypes. Among the derivatives studied, (±)-3-methoxy-1-oxa-2,7-diaza-7,10-ethanospiro-[4.5]dec-2-ene sesquifumarate **6a** was characterized as a high affinity α7 nAChR partial agonist with relevant α7 versus α4β2 selectivity in both binding and functional experiments. Moreover, derivative **6a** did not bind significantly to α3β4 or α1β1γδ nAChRs and to the five mAChRs, and marginally activated human 5-HT_3 receptors expressed in cell lines. We prepared the two enantiomers of (±)-**6a** by a resolution protocol, assigned absolute R configuration to the eutomer by X-ray analysis, and determined the enantioselectivity ratio (*R*)-**6a**/(*S*)-**6a** at rat as well as at human α7 nAChR subtypes. At present, pharmacokinetic profiling of (±)-**6a** is under evaluation, as well as the in vivo activity in animal models to assess applica-

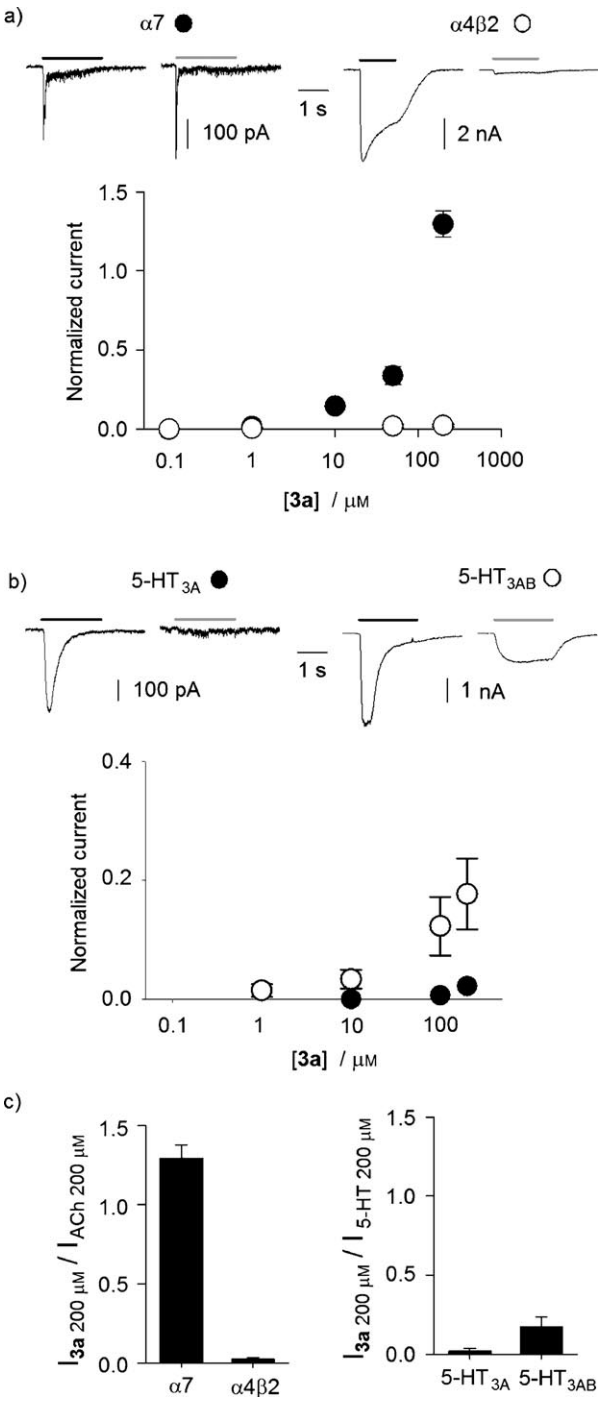

Figure 4. Effects of **3a** on different types of human ligand-gated receptors. a) (top) Typical traces evoked by ACh (black bar, 200 μM) or **3a** (gray bar, 200 μM) in GH4C1 cells stably transfected with human α7 nAChR subunit (●) or on HEK 293 cells stably transfected with human α4 and β2 nAChR subunits (○), as indicated. Cells were held at −70 mV; (bottom) **3a** dose-normalized response relationship for human α7 nAChR (●, $n=6$) and for human α4β2 nAChR (○, $n=7$); b) (top) typical traces evoked by 200 μM 5-HT or 200 μM **3a** in GH4C1 cells transiently transfected with human 5-HT_{3A} subunit (●) or with human 5-HT_{3A} and 5-HT_{3B} subunits (○), as indicated; (bottom) **3a** dose-normalized response relationship for human 5-HT_{3A} receptors (●, $n=5$) and for human 5-HT_{3AB} receptors (○, $n=5$); c) histograms showing the ratio between the mean current amplitude evoked by 200 μM **3a** and 200 μM ACh on nicotinic receptors (left, as indicated) or 200 μM 5-HT on 5-HT_3 receptors (right, as indicated).

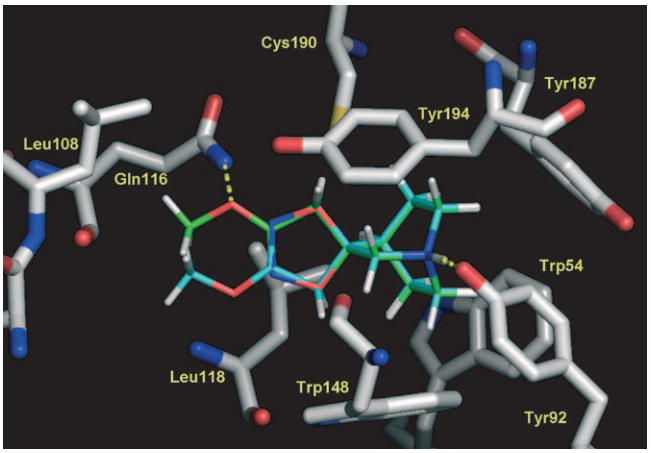

Figure 5. Binding modes of (*R*)-**6** and (*S*)-**6** in the active site of α7 nAChR. Receptor model residues are depicted as a stick model with carbon atoms colored in gray. The carbon atoms of (*R*)-**6** and (*S*)-**6** are green and cyan, respectively. Some residues have been omitted for clarity.

bility of this compound to treat CNS cognitive diseases and neuropathic pain.

Experimental Section

Chemistry

Materials and methods: Alkene **13**,[24] ethyl 2-chloro-2-(hydroximino)-acetate,[25] dibromoformaldoxime,[27a] and 1-chloroacetaldoxime[27b] were prepared according to literature procedures. ^{1}H NMR and ^{13}C NMR spectra were recorded with a Varian Mercury 300 (^{1}H: 300.063; ^{13}C: 75.451 MHz) spectrometer at 20 °C. Chemical shifts (δ) are expressed in ppm, with coupling constants (*J*) in Hz. TLC analyses were performed on commercial silica gel 60 F_{254} aluminum sheets; spots were further evidenced by spraying with a dilute alkaline potassium permanganate solution or, for tertiary amines, with Dragendorff reagent. Melting points were determined on a model B 540 Büchi apparatus and are uncorrected. Rotary power determinations (sodium D line, 589 nm) were carried out with a Jasco P-1010 polarimeter coupled with a Huber thermostat. Chiral HPLC analyses were performed with a Jasco PU-980 pump equipped with a UV-Vis detector (Jasco UV-975) using a Daicel Chiralpak AD column (0.46 cm × 25 cm). Microanalyses (C, H, N) agreed with theoretical values within ±0.4%.

(±)-3-Ethyl-1-oxa-2,7-diaza-7,10-ethanospiro[4.5]dec-2-ene carboxylate (1): A solution of ethyl 2-chloro-2-(hydroximino)-acetate (2.46 g, 16.24 mmol) in dioxane (40 mL) was added to a magnetically stirred suspension of **13** (1.0 g, 8.12 mmol) and $NaHCO_3$ (6.82 g, 81.2 mmol) in dioxane (50 mL). The reaction mixture was heated at reflux for 4 d with further addition of ethyl 2-chloro-2-(hydroximino)-acetate (2.46 g, 16.24 mmol) in dioxane (40 mL). After filtration and removal of the solvent at reduced pressure, the residue was purified by silica gel column chromatography (CH_2Cl_2/MeOH, 9:1) to afford cycloadduct **1** (251 mg, 13%) as a pale yellow viscous oil: $R_f=0.67$ (CH_2Cl_2/MeOH, 4:1); ^{1}H NMR (300 MHz, $CDCl_3$): $\delta=1.29$ (t, $J=7.0$, 3H), 1.42 (m, 1H), 1.60 (m, 2H), 1.91 (br s, 1H), 2.07 (m, 1H), 2.75 (m, 2H), 2.87 (m, 3H), 2.91 (d, $J=18.3$, 1H), 3.22 (d, $J=15.3$, 1H), 3.27 (d, $J=18.3$, 1H), 4.27 ppm (q, $J=7.0$, 2H); ^{13}C NMR (75 MHz, $CDCl_3$): $\delta=14.4$, 21.3, 23.6, 31.3, 43.4, 46.6, 47.0,

62.2, 63.2, 90.6, 150.7, 161.1 ppm; Anal. calcd for $C_{12}H_{18}N_2O_3$: C 60.49, H 7.61, N 11.76, found: C 60.80, H 7.28, N 12.03.

(±)-3-Hydroxymethyl-1-oxa-2,7-diaza-7,10-ethanospiro[4.5]dec-2-ene (2): $NaBH_4$ (480 mg, 12.69 mmol) was added portionwise to a magnetically stirred solution of ester **1** (400 mg, 1.68 mmol) in EtOH (10 mL) at RT. After 5 h, 5 mL of 2 N HCl were added (pH ≈ 3), the solvent was evaporated, and the acidic residue was extracted with EtOAc (3×5 mL). The residual aqueous phase, basified by portionwise addition of K_2CO_3, was then repeatedly extracted with CH_2Cl_2 (15×5 mL). The pooled organic phases were dried over anhyd Na_2SO_4, then filtered and concentrated in vacuo to provide the primary alcohol **2** (158 mg, 48%) as a yellow viscous oil: R_f = 0.27 (CH_2Cl_2/MeOH, 4:1); ^{1}H NMR (300 MHz, CD_3OD): δ = 1.57 (m, 1H), 1.72 (m, 2H), 1.93 (m, 1H), 2.09 (m, 1H), 2.74–2.88 (m, 4H), 2.92 (d, J = 17.9, 1H), 3.03 (d, J = 15.0, 1H), 3.09 (d, J = 15.0, 1H), 3.25 (d, J = 17.9, 1H), 4.26 ppm (s, 2H); ^{13}C NMR (75 MHz, $CDCl_3$): δ = 21.5, 23.8, 31.2, 45.0, 46.6, 46.9, 58.6, 63.5, 86.8, 157.9 ppm; Anal. calcd for $C_{10}H_{16}N_2O_2$: C 61.20, H 8.22, N 14.27, found: C 60.92, H 8.51, N 14.46.

Borane-3-methylene-1-azabicyclo[2.2.2]octane complex (14): A 1.0 M solution of BH_3·THF (18 mL) was added under nitrogen to a stirred solution of **13** (2.20 g, 17.9 mmol) in dry THF (10 mL) at 0 °C. After 30 min, the mixture was concentrated in vacuo and the residue was purified by silica gel column chromatography (PE/EtOAc, 9:1) to yield **14** as a colorless solid (2.05 g, 84%), which was crystallized from *n*-hexane/Et_2O (mp 70–72 °C, literature:[26] 72–73 °C): R_f = 0.64 (PE/EtOAc, 4:1); ^{1}H NMR (300 MHz, $CDCl_3$): δ = 1.86 (m, 4H), 2.56 (m, 1H), 3.04 (m, 4H), 3.63 (br s, 2H), 4.74 (br s, 1H), 4.91 ppm (br s, 1H); ^{13}C NMR (75 MHz, $CDCl_3$): δ = 26.4, 31.4, 54.1, 61.2, 106.7, 144.7 ppm.

(±)-3-Bromo-1-oxa-2,7-diaza-7-boranyl-7,10-ethanospiro[4.5]dec-2-ene (15): Dibromoformaldoxime (6.66 g, 32.8 mmol) was added to a suspension of **14** (4.50 g, 32.8 mmol) and K_2CO_3 (22.7 g, 164 mmol) in EtOAc (90 mL). The reaction mixture was stirred at RT for five days with further addition of dibromoformaldoxime (5× 2.67 g). After completion of the cycloaddition, Celite® was added, and the resulting slurry was filtered under vacuum and washed with EtOAc. The solvent was evaporated, and the residue was purified by silica gel column chromatography (PE/EtOAc, 1:1) to afford cycloadduct **15** (4.05 g, 48%), which crystallized as colorless prisms from EtOAc (mp 127–128 °C): R_f = 0.18 (PE/EtOAc, 2:3); ^{1}H NMR (300 MHz, $CDCl_3$): δ = 1.73 (m, 2H), 1.98 (m, 1H), 2.25 (br s, 1H), 2.33 (m, 1H), 2.98–3.18 (m, 5H), 3.13 (d, J = 17.2, 1H), 3.32 (d, J = 17.2, 1H), 3.40 ppm (dd, J = 1.8 and 14.6, 1H); ^{13}C NMR (75 MHz, $CDCl_3$): δ = 20.1, 22.1, 30.7, 51.1, 51.7, 52.5, 65.5, 85.8, 136.4 ppm; Anal. calcd for $C_9H_{16}BBrN_2O$: C 41.74, H 6.23, N 10.82, found: C 41.60, H 6.47, N 11.07.

(±)-3-Methyl-1-oxa-2,7-diaza-7-boranyl-7,10-ethanospiro-[4.5]dec-2-ene (16): A solution of 1-chloroacetaldoxime (1.02 g, 10.96 mmol) in CH_2Cl_2 (5 mL) and Et_3N (1.5 mL, 10.96 mmol) was added to a solution of **14** (1.0 g, 7.30 mmol) in CH_2Cl_2 (50 mL). The reaction mixture was stirred at RT for 2 d with further addition of 1-chloroacetaldoxime (5×1.02 g) and Et_3N (5×1.5 mL). After completion of cycloaddition, the solvent was evaporated, and the residue was diluted with H_2O (30 mL) and extracted with CH_2Cl_2 (3× 30 mL). The combined organic layers were dried over anhyd Na_2SO_4, then filtered and concentrated in vacuo. After silica gel column chromatography (PE/EtOAc, 4:1), Δ^2-isoxazoline **16** (430 mg, 30%) was obtained as a pale yellow oil: R_f = 0.30 (PE/EtOAc, 2:3); ^{1}H NMR (300 MHz, $CDCl_3$): δ = 1.68 (m, 2H), 1.86 (m, 1H), 1.99 (s, 3H), 2.05 (br s, 1H), 2.28 (m, 1H), 2.77 (d, J = 17.2, 1H), 2.91–3.09 (m, 5H), 3.02 (d, J = 17.2, 1H), 3.37 ppm (dd, J = 2.5 and 14.6, 1H); ^{13}C NMR (75 MHz, $CDCl_3$): δ = 13.3, 20.5, 23.3, 30.7, 48.5, 51.2, 52.3, 63.3, 84.7, 154.2 ppm; Anal. calcd for $C_{10}H_{19}BN_2O$: C 61.88, H 9.87, N 14.43, found: C 61.55, H 10.18, N 14.62.

(±)-3-Phenyl-1-oxa-2,7-diaza-7-boranyl-7,10-ethanospiro[4.5]dec-2-ene (17): NaClO (4 mL, 10% aq solution) was added dropwise to a solution of **14** (500 mg, 3.65 mmol) and benzaldoxime (624 mg, 5.48 mmol) in CH_2Cl_2 (5 mL). The reaction mixture was stirred at RT for 5 d with further addition of benzaldoxime (5× 500 mg) and NaClO (5×4 mL, 10% aqueous solution). The phases were separated and the aqueous layer was extracted with CH_2Cl_2 (3×10 mL). After standard workup, the residue was purified by silica gel column chromatography (PE/EtOAc, 7:3) to afford cycloadduct **17** (150 mg, 16%), which crystallized as colorless prisms from EtOAc (mp 181–183 °C): R_f = 0.23 (PE/EtOAc, 7:3); ^{1}H NMR (300 MHz, $CDCl_3$): δ = 1.81 (m, 2H), 2.03 (m, 1H), 2.29 (m, 1H), 2.45 (m, 1H), 3.17–3.48 (m, 5H), 3.27 (d, J = 17.2, 1H), 3.50 (d, J = 17.2, 1H), 3.68 (dd, J = 2.2 and 14.3, 1H), 7.43 (m, 3H), 7.65 ppm (m, 2H); ^{13}C NMR (75 MHz, $CDCl_3$): δ = 20.2, 22.0, 31.5, 45.2, 47.8, 49.5, 62.2, 84.6, 126.7, 129.0, 130.7, 156.0 ppm; Anal. calcd for $C_{15}H_{21}BN_2O$: C 70.33, H 8.26, N 10.94, found: C 70.59, H 8.38, N 10.71.

(±)-3-Methoxy-1-oxa-2,7-diaza-7-boranyl-7,10-ethanospiro[4.5]dec-2-ene (18): A stirred suspension of bromo-Δ^2-isoxazoline **15** (1.00 g, 3.86 mmol) and K_2CO_3 (5.34 g, 38.6 mmol) in MeOH (60 mL) was stirred at RT for 16 h. After addition of Celite® and filtration under vacuum, the crude filtrate was submitted to silica gel column chromatography (PE/EtOAc, 1:4), affording desired methoxy derivative **18** (654 mg, 81%) as colorless prisms from EtOAc/Et_2O; mp 108.5–110 °C; R_f = 0.34 (PE/EtOAc, 1:4); ^{1}H NMR (300 MHz, $CDCl_3$): δ = 1.70 (m, 2H), 1.96 (m, 1H), 2.27 (br s, 1H), 2.34 (m, 1H), 2.86 (d, J = 16.5, 1H), 2.95–3.14 (m, 6H), 3.37 (dd, J = 2.2 and 14.3, 1H), 3.85 ppm (s, 3H); ^{13}C NMR (75 MHz, $CDCl_3$): δ = 20.2, 22.3, 30.5, 42.5, 51.8, 52.5, 57.7, 65.8, 84.5, 166.6 ppm; Anal. calcd for $C_{10}H_{19}BN_2O_2$: C 57.17, H 9.12, N 13.33, found: C 56.95, H 9.31, N 13.59.

(±)-3-Ethoxy-1-oxa-2,7-diaza-7-boranyl-7,10-ethanospiro[4.5]dec-2-ene (19): The title compound, prepared by the procedure described for analogue **18** using EtOH as a solvent, was obtained as colorless prisms in 61% yield from EtOAc/*n*-hexane; mp 94–95 °C; R_f = 0.44 (PE/EtOAc, 1:4); ^{1}H NMR (300 MHz, $CDCl_3$): δ = 1.34 (t, J = 7.0, 3H), 1.68 (m, 2H), 1.93 (m, 1H), 2.25 (br s, 1H), 2.33 (m, 1H), 2.85 (d, J = 16.5, 1H), 2.95–3.08 (m, 5H), 3.10 (d, J = 16.5, 1H), 3.36 (d, J = 14.3, 1H), 4.16 ppm (q, J = 7.0, 2H); ^{13}C NMR (75 MHz, $CDCl_3$): δ = 14.8, 20.2, 22.3, 30.4, 42.8, 51.8, 52.4, 65.8, 66.6, 84.1, 165.9 ppm; Anal. calcd for $C_{11}H_{21}BN_2O_2$: C 58.95, H 9.44, N 12.50, found: C 58.88, H 9.67, N 12.23.

(±)-3-*n*-Propoxy-1-oxa-2,7-diaza-7-boranyl-7,10-ethanospiro[4.5]dec-2-ene (20): NaH (188 mg, 7.82 mmol) was added to a stirred solution of *n*-propanol (0.54 mL, 7.11 mmol) in anhyd THF under nitrogen at 0 °C. After 30 min, a solution of **15** (920 mg, 3.55 mmol) in anhyd THF was added dropwise and the mixture was stirred at RT for 16 h. After addition of H_2O (1 mL), the solvent was concentrated in vacuo, and the residue was diluted with H_2O (5 mL) and extracted with EtOAc (4×5 mL). After the usual workup, the crude reaction mixture was purified by silica gel column chromatography (PE/EtOAc, 2:3) to afford **20** (600 mg, 71%) as a colorless, viscous oil: R_f = 0.53 (PE/EtOAc, 2:3); ^{1}H NMR (300 MHz, $CDCl_3$): δ = 0.96 (t, J = 7.3, 3H), 1.72 (m, 4H), 1.94 (m, 1H), 2.25 (br s, 1H), 2.33 (m, 1H), 2.86 (d, J = 16.5, 1H), 2.95–3.12 (m, 5H), 3.04 (d, J = 16.5, 1H), 3.35 (dd, J = 1.8 and 14.3, 1H), 4.06 ppm (t, J = 6.6, 2H); ^{13}C NMR

(75 MHz, $CDCl_3$): $\delta = 10.2$, 19.7, 21.9, 22.0, 30.0, 42.3, 51.4, 52.0, 65.4, 71.8, 83.6, 165.7 ppm; Anal. calcd for $C_{12}H_{23}BN_2O_2$: C 60.52, H 9.74, N 11.76, found: C 60.35, H 10.07, N 11.58.

(±)-3-Benzyloxy-1-oxa-2,7-diaza-7-boranyl-7,10-ethanospiro[4.5]dec-2-ene (21): The title compound, prepared by the procedure described for analogue **20** using benzyl alcohol, was obtained in 77% yield as colorless prisms from EtOAc/*n*-hexane; mp 128–129 °C; $R_f = 0.44$ (PE/EtOAc, 2:3); ^{1}H NMR (300 MHz, $CDCl_3$): $\delta = 1.70$ (m, 2H), 1.94 (m, 1H), 2.28 (br s, 1H), 2.35 (m, 1H), 2.92 (d, $J = 16.5$, 1H), 2.96–3.14 (m, 6H), 3.39 (dd, $J = 1.8$ and 14.6, 1H), 5.13 (s, 2H), 7.37 ppm (m, 5H); ^{13}C NMR (75 MHz, $CDCl_3$): $\delta = 20.2$, 22.3, 30.5, 42.7, 51.7, 52.4, 65.8, 72.4, 84.4, 128.7, 128.9, 129.0, 135.1, 165.8 ppm; Anal. calcd for $C_{16}H_{23}BN_2O_2$: C 67.15, H 8.10, N 9.79, found: C 67.06, H 8.37, N 9.95.

(±)-3-Propargyloxy-1-oxa-2,7-diaza-7-boranyl-7,10-ethanospiro-[4.5]dec-2-ene (22): The title compound, prepared by the procedure described for analogue **20** using propargyl alcohol, was obtained as colorless prisms in 74% yield from EtOAc/*n*-hexane; mp 127–129 °C; $R_f = 0.48$ (PE/EtOAc, 3:7); ^{1}H NMR (300 MHz, $CDCl_3$): $\delta =$ 1.68 (m, 2H), 1.95 (m, 1H), 2.28 (br s, 1H), 2.35 (m, 1H), 2.61 (t, $J =$ 2.2, 1H), 2.91 (d, $J = 16.5$, 1H), 2.95–3.11 (m, 5H), 3.09 (d, $J = 16.5$, 1H), 3.39 (dd, $J = 1.8$ and 14.3, 1H), 4.75 ppm (d, $J = 2.2$, 2H); ^{13}C NMR (75 MHz, $CDCl_3$): $\delta = 19.1$, 21.6, 30.2, 42.5, 51.3, 52.1, 58.1, 65.4, 80.5, 84.6, 165.7, 167.3 ppm; Anal. calcd for $C_{12}H_{19}BN_2O_2$: C 61.57, H 8.18, N 11.97, found: C 61.80, H 8.35, N 11.71.

(±)-1-Oxa-2,7-diaza-7-boranyl-7,10-ethanospiro[4.5]decan-3-one (23): A suspension of benzyloxy derivative **21** (450 mg, 1.57 mmol) and 10% Pd/C (45 mg) in MeOH (10 mL) was stirred under hydrogen at atmospheric pressure for 5 h. The reaction mixture was filtered and the solvent was evaporated in vacuo to afford **23** (298 mg, 97%) as a colorless oil: $R_f = 0.23$ (CH_2Cl_2/MeOH, 95:5); ^{1}H NMR (300 MHz, $CDCl_3$): $\delta = 1.72$ (m, 2H), 1.96 (m, 2H), 2.20 (m, 1H), 2.38 (br s, 1H), 2.74 (d, $J = 16.5$, 1H), 2.84 (d, $J = 16.5$, 1H), 2.92–3.08 (m, 4H), 3.13 (d, $J = 14.3$, 1H), 3.34 ppm (d, $J = 14.3$, 1H); ^{13}C NMR (75 MHz, $CDCl_3$): $\delta = 19.4$, 21.4, 29.1, 41.6, 51.5, 51.9, 63.5, 83.2, 172.6 ppm; Anal. calcd for $C_9H_{17}BN_2O_2$: C 55.14, H 8.74, N 14.29, found: C 55.48, H 8.48, N 13.97.

(±)-2-Methyl-1-oxa-2,7-diaza-7-boranyl-7,10-ethanospiro[4.5]decan-3-one (24): Excess CH_3I (1.5 mL) was added to a suspension of isoxazolidin-3-one **23** (900 mg, 4.59 mmol) and K_2CO_3 (1.90 g, 13.75 mmol) in acetone (30 mL). After stirring at RT for 16 h, the solvent was evaporated, and the residue was diluted with H_2O (10 mL) and extracted with CH_2Cl_2 (4×10 mL). After standard workup, the crude reaction mixture was purified by silica gel column chromatography (CH_2Cl_2/MeOH, 95:5) to afford N-methylated compound **24** (850 mg, 88%) as a colorless oil: $R_f = 0.51$ (CH_2Cl_2/MeOH, 95:5); ^{1}H NMR (300 MHz, $CDCl_3$): $\delta = 1.71$ (m, 2H), 1.97 (m, 1H), 2.22 (m, 1H), 2.33 (br s, 1H), 2.70 (d, $J = 16.5$, 1H), 2.84 (d, $J = 16.5$, 1H), 2.95–3.14 (m, 4H), 3.16 (s, 3H), 3.28 (dd, $J =$ 2.2 and 15.0, 1H), 3.36 ppm (dd, $J = 2.2$ and 15.0, 1H); ^{13}C NMR (75 MHz, $CDCl_3$): $\delta = 20.0$, 21.7, 29.6, 32.4, 42.5, 51.9, 52.4, 64.3, 80.3, 168.1 ppm; Anal. calcd for $C_{10}H_{19}BN_2O_2$: C 57.17, H 9.12, N 13.33, found: C 57.40, H 9.31, N 12.95.

(±)-3-Bromo-1-oxa-2,7-diaza-7,10-ethanospiro[4.5]dec-2-ene (3): A solution of CF_3CO_2H (1 mL) in acetone (5 mL) was added dropwise to an ice-cooled, stirred solution of **15** (640 mg, 2.47 mmol) in acetone (7 mL). After disappearance of the starting material, which was monitored by TLC (PE/EtOAc, 1:4), toluene (5 mL) was added, and the solvents and excess reagent were evaporated in vacuo. The residue was diluted with H_2O (5 mL) and extracted with Et_2O (3×5 mL). The residual aqueous phase was basified by portionwise addition of K_2CO_3 and extracted with CH_2Cl_2 (4×5 mL). After standard workup, the tertiary base **3** (459 mg, 76%) was obtained as a colorless oil: $R_f = 0.57$ (CH_2Cl_2/MeOH, 9:1); ^{1}H NMR (300 MHz, $CDCl_3$): $\delta = 1.50$ (m, 2H), 1.69 (1H, m), 2.01 (m, 1H), 2.12 (m, 1H), 2.68–2.92 (m, 4H), 2.97 (d, $J = 14.4$, 1H), 3.00 (d, $J = 17.3$,1H), 3.29 (d, $J = 14.4$, 1H), 3.31 ppm (d, $J = 17.3$, 1H); ^{13}C NMR (75 MHz, $CDCl_3$): $\delta = 20.9$, 23.3, 31.0, 46.4, 46.8, 51.2, 62.7, 88.1, 136.2 ppm; Anal. calcd for $C_9H_{13}BrN_2O$: C 44.10, H 5.35, N 11.43, found: C 44.38, H 5.11, N 11.09.

(±)-3-Methyl-1-oxa-2,7-diaza-7,10-ethanospiro[4.5]dec-2-ene (4): The title compound was prepared starting from **16** (311 mg, 1.60 mmol) using the protocol described for **3**. After standard workup, tertiary amine **4** (193 mg, 67%) was obtained as a yellow oil: $R_f = 0.38$ (CH_2Cl_2/MeOH, 4:1); ^{1}H NMR and ^{13}C NMR data matched those found in the literature.[24]

(±)-3-Phenyl-1-oxa-2,7-diaza-7,10-ethanospiro[4.5]dec-2-ene (5): The title compound was prepared starting from **17** (150 mg, 0.586 mmol) using the protocol described for **3**. After standard workup, tertiary amine **5** (50 mg, 35%) was obtained as a colorless, viscous oil: $R_f = 0.30$ (CH_2Cl_2/MeOH, 95:5); ^{1}H NMR and ^{13}C NMR data matched those found in the literature.[24]

(±)-3-Methoxy-1-oxa-2,7-diaza-7,10-ethanospiro[4.5]dec-2-ene (6): The title compound was prepared starting from **18** (640 mg, 3.05 mmol) using the protocol described for **3**. After standard workup, the desired reaction product **6** (403 mg, 67%) was obtained as a colorless oil: $R_f = 0.30$ (CH_2Cl_2/MeOH, 95:5); ^{1}H NMR (300 MHz, $CDCl_3$): $\delta = 1.50$ (m, 1H), 1.61 (m, 1H), 1.75 (m, 1H), 2.11 (br s, 1H), 2.23 (m, 1H), 2.80 (d, $J = 16.5$, 1H), 2.87–3.05 (m, 5H), 3.07 (d, $J = 16.5$, 1H), 3.33 (dd, $J = 1.8$ and 14.3, 1H), 3.84 ppm (s, 3H); ^{13}C NMR (75 MHz, $CDCl_3$): $\delta = 21.0$, 23.6, 30.9, 42.6, 46.7, 47.0, 57.3, 62.7, 86.5, 166.9 ppm; Anal. calcd for $C_{10}H_{16}N_2O_2$: C 61.16, H 8.22, N 14.27, found: C 61.45, H 8.49, N 13.92.

(±)-3-Ethoxy-1-oxa-2,7-diaza-7,10-ethanospiro[4.5]dec-2-ene (7): The title compound was prepared starting from **19** (450 mg, 2.01 mmol) using the protocol described for **3**. After standard workup, amine **7** (288 mg, 68%) was obtained as a colorless oil: $R_f = 0.33$ (CH_2Cl_2/MeOH, 95:5); ^{1}H NMR (300 MHz, $CDCl_3$): $\delta = 1.33$ (t, $J = 7.0$, 3H), 1.42 (m, 1H), 1.54 (m, 1H), 1.64 (m, 1H), 2.02 (m, 1H), 2.12 (m, 1H), 2.75 (d, $J = 16.5$, 1H), 2.78–2.90 (m, 4H), 2.94 (dd, $J =$ 2.2 and 14.7, 1H), 3.03 (d, $J = 16.5$, 1H), 3.24 (dd, $J = 2.2$ and 14.7, 1H), 4.15 ppm (q, $J = 7.0$, 2H); ^{13}C NMR (75 MHz, $CDCl_3$): $\delta = 14.8$, 21.3, 24.0, 31.0, 42.9, 46.8, 47.1, 63.1, 66.0, 86.4, 166.2 ppm; Anal. calcd for $C_{11}H_{18}N_2O_2$: C 62.83, H 8.63, N 13.32, found: C 62.58, H 8.31, N 13.55.

(±)-3-*n*-Propoxy-1-oxa-2,7-diaza-7,10-ethanospiro[4.5]dec-2-ene (8): The title compound was prepared starting from **20** (590 mg, 2.48 mmol) using the protocol described for **3**. After standard workup, the reaction product **8** (450 mg, 81%) was obtained as a colorless oil: $R_f = 0.42$ (CH_2Cl_2/MeOH, 95:5); ^{1}H NMR (300 MHz, $CDCl_3$): $\delta = 0.95$ (t, $J = 7.3$, 3H), 1.37 (m, 1H), 1.48 (m, 1H), 1.64 (m, 1H), 1.70 (m, 2H), 2.03 (m, 1H), 2.08 (m, 1H), 2.75 (d, $J = 16.5$, 1H), 2.74–2.88 (m, 4H), 2.95 (dd, $J = 1.8$ and 14.6, 1H), 3.03 (d, $J = 16.5$, 1H), 3.22 (dd, $J = 1.8$ and 14.6, 1H), 4.05 ppm (t, $J = 6.6$, 2H); ^{13}C NMR (75 MHz, $CDCl_3$): $\delta = 10.3$, 20.9, 22.1, 23.6, 30.5, 42.4, 46.4, 46.6, 62.7, 71.2, 85.9, 166.0 ppm; Anal. calcd for $C_{12}H_{20}N_2O_2$: C 64.26, H 8.99, N 12.49, found: C 63.86, H 8.70, N 12.76.

(±)-3-Benzyloxy-1-oxa-2,7-diaza-7,10-ethanospiro[4.5]dec-2-ene (9): The title compound was prepared starting from **21** (350 mg, 1.22 mmol) using the protocol described for **3**. After standard workup, the desired reaction product **9** (264 mg, 79%) was ob-

tained as a pale yellow oil: $R_f = 0.25$ (CH_2Cl_2/MeOH, 95:5); ^1H NMR (300 MHz, $CDCl_3$): $\delta = 1.41$ (m, 1H), 1.54 (m, 1H), 1.63 (m, 1H), 2.05 (br s, 1H), 2.14 (m, 1H), 2.72–2.91 (m, 4H), 2.78 (d, $J = 16.1$, 1H), 2.96 (d, $J = 14.3$, 1H), 3.09 (d, $J = 16.1$, 1H), 3.26 (d, $J = 14.3$, 1H), 5.12 (s, 2H), 7.38 ppm (m, 5H); ^{13}C NMR (75 MHz, $CDCl_3$): $\delta = 20.5$, 23.6, 30.5, 42.1, 46.3, 47.1, 62.5, 71.5, 86.0, 128.5, 128.9, 129.1, 135.6, 165.8 ppm; Anal. calcd for $C_{16}H_{20}N_2O_2$: C 70.56, H 7.40, N 10.29, found: C 70.32, H 7.64, N 10.53.

(±)-3-*n*-Propargyloxy-1-oxa-2,7-diaza-7,10-ethanospiro[4.5]dec-2-ene (10): The title compound was prepared starting from **22** (278 mg, 1.19 mmol) using the protocol described for **3**. After standard workup, the reaction product **10** (178 mg, 68%) was obtained as a colorless oil: $R_f = 0.25$ (CH_2Cl_2/MeOH, 95:5); ^1H NMR (300 MHz, $CDCl_3$): $\delta = 1.47$ (m, 2H), 1.65 (m, 1H), 2.04 (br s, 1H), 2.11 (m, 1H), 2.58 (t, $J = 1.5$, 1H), 2.70–2.90 (m, 5H), 2.95 (d, $J = 14.6$, 1H), 3.09 (d, $J = 16.5$, 1H), 3.25 (d, $J = 14.6$, 1H), 4.74 ppm (d, $J = 1.5$, 2H); ^{13}C NMR (75 MHz, $CDCl_3$): $\delta = 19.1$, 21.6, 30.2, 42.5, 46.4, 46.6, 58.1, 62.6, 85.8, 86.0, 167.3, 168.1 ppm; Anal. calcd for $C_{12}H_{16}N_2O_2$: C 65.43, H 7.32, N 12.72, found: C 65.12, H 7.45, N 12.47.

(±)-1-Oxa-2,7-diaza-7,10-ethanospiro[4.5]decan-3-one (11): The title compound was prepared starting from **23** (400 mg, 2.04 mmol) using the protocol described for **3**. After standard workup, the desired tertiary amine **11** (202 mg, 54%) was obtained as a yellow oil: $R_f = 0.18$ (CH_2Cl_2/MeOH, 9:1); ^1H NMR (300 MHz, $CDCl_3$): $\delta = 1.46$ (m, 2H), 1.60 (m, 1H), 1.95 (m, 1H), 2.03 (br s, 1H), 2.54 (d, $J = 16.1$, 1H), 2.58–2.95 (m, 7H), 3.08 ppm (d, $J = 14.6$, 1H); ^{13}C NMR (75 MHz, $CDCl_3$): $\delta = 20.8$, 23.5, 29.0, 43.0, 46.8, 48.2, 62.1, 82.9, 168.5 ppm; Anal. calcd for $C_9H_{14}N_2O_2$: C 59.32, H 7.74, N 15.37, found: C 59.66, H 7.38, N 15.02.

(±)-2-Methyl-1-oxa-2,7-diaza-7,10-ethanospiro[4.5]decan-3-one (12): The title compound was prepared starting from **24** (500 mg, 2.38 mmol) using the protocol described for **3**. After standard workup, the reaction product **12** (271 mg, 58%) was obtained as a colorless oil: $R_f = 0.31$ (CH_2Cl_2/MeOH, 9:1); ^1H NMR (300 MHz, $CDCl_3$): $\delta = 1.47$ (m, 1H), 1.54 (m, 1H), 1.69 (m, 1H), 2.01 (m, 1H), 2.08 (br s, 1H), 2.59 (d, $J = 16.1$, 1H), 2.72–2.88 (m, 5H), 2.93 (d, $J = 16.1$, 1H), 3.14 (s, 3H), 3.15 ppm (dd, $J = 2.2$ and 14.3, 1H); ^{13}C NMR (75 MHz, $CDCl_3$): $\delta = 20.9$, 23.4, 30.0, 32.1, 42.6, 46.7, 47.2, 61.8, 82.8, 168.9 ppm; Anal. calcd for $C_{10}H_{16}N_2O_2$: C 61.20, H 8.22, N 14.27, found: C 60.93, H 8.38, N 14.52.

General procedure for the preparation of fumarates: A solution of fumaric acid (102 mg, 0.88 mmol) in MeOH (2 mL) was added to a solution of the free base (0.8 mmol) in MeOH (3 mL). After stirring overnight at RT, the solvent was removed at reduced pressure, and the crude salt was obtained quantitatively.

(±)-3-Ethoxycarbonyl-1-oxa-2,7-diaza-7,10-ethanospiro[4.5]dec-2-ene fumarate 1×1.5 $C_4H_4O_4$ (1a): Colorless prisms; mp: 164–166 °C (abs EtOH); ^1H NMR (300 MHz, CD_3OD): $\delta = 1.33$ (t, $J = 7.0$, 3H), 1.96 (m, 3H), 2.32 (m, 2H), 3.20–3.42 (m, 5H), 3.51 (d, $J = 18.0$, 1H), 3.57 (dd, $J = 2.2$ and 13.9, 1H), 3.62 (dd, $J = 2.2$ and 13.9, 1H), 4.33 (q, $J = 7.0$, 2H), 6.69 ppm (s, 3H); ^{13}C NMR (75 MHz, D_2O): $\delta = 13.3$, 17.6, 19.2, 29.4, 42.4, 45.9, 46.5, 58.8, 63.4, 87.6, 134.9, 152.8, 161.3, 171.6 ppm; Anal. calcd for $C_{18}H_{24}N_2O_9$: C 52.42, H 5.87, N 6.79, found: C 52.18, H 6.05, N 7.05.

(±)-3-Hydroxymethyl-1-oxa-2,7-diaza-7,10-ethanospiro[4.5]dec-2-ene fumarate 2×$C_4H_4O_4$ (2a): Colorless prisms; mp: 180–182 °C, dec. (abs EtOH); ^1H NMR (300 MHz, D_2O): $\delta = 1.75$ (m, 2H), 1.89 (m, 1H), 2.08 (m, 1H), 2.14 (br s, 1H), 2.99 (d, $J = 17.9$, 1H), 3.03–3.29 (m, 4H), 3.22 (d, $J = 17.9$, 1H), 3.38 (dd, $J = 1.9$ and 14.3, 1H), 3.45 (dd, $J = 1.9$ and 14.3, 1H), 4.18 (s, 2H), 6.49 ppm (s, 2H); ^{13}C NMR (75 MHz, D_2O): $\delta = 17.8$, 19.4, 29.2, 44.1, 45.9, 46.4, 56.6, 58.9, 83.9, 134.8, 160.7, 171.5 ppm; Anal. calcd for $C_{14}H_{20}N_2O_6$: C 53.84, H 6.45, N 8.97, found: C 53.97, H 6.12, N 8.64.

(±)-3-Bromo-1-oxa-2,7-diaza-7,10-ethanospiro[4.5]dec-2-ene fumarate 3×0.5 $C_4H_4O_4$ (3a): Colorless prisms; mp: 145–146 °C (2-propanol/EtOAc); ^1H NMR (300 MHz, D_2O): $\delta = 1.73$ (m, 2H), 1.88 (m, 1H), 2.11 (m, 1H), 2.22 (br s, 1H), 3.09 (m, 3H), 3.20 (m, 1H), 3.23 (d, $J = 18.2$, 1H), 3.41 (dd, $J = 2.3$ and 14.4, 1H), 3.44 (d, $J = 18.2$, 1H), 3.49 (dd, $J = 2.3$ and 14.4, 1H), 6.40 ppm (s, 1H); ^{13}C NMR (75 MHz, D_2O): $\delta = 17.5$, 19.1, 29.1, 45.8, 46.4, 49.8, 58.7, 85.4, 135.1, 139.8, 172.7 ppm; Anal. calcd for $C_{11}H_{15}BrN_2O_3$: C 43.58, H 4.99, N 9.24, found: C 43.38, H 5.15, N 9.07.

(±)-3-Methyl-1-oxa-2,7-diaza-7,10-ethanospiro[4.5]dec-2-ene fumarate 4×0.75 $C_4H_4O_4$ (4a): Pale yellow powder; mp: 172–173 °C dec. (EtOAc/*n*-hexane/2-propanol); ^1H NMR (300 MHz, D_2O): $\delta = 1.74$ (m, 2H), 1.81 (s, 3H), 1.88 (m, 1H), 2.08 (m, 1H), 2.12 (m, 1H), 2.95 (d, $J = 17.9$, 1H), 3.13 (m, 3H), 3.23 (m, 2H), 3.38 (dd, $J = 2.2$ and 14.3, 1H), 3.43 (dd, $J = 2.2$ and 14.3, 1H), 6.48 ppm (s, 1.5H); ^{13}C NMR (75 MHz, D_2O): $\delta = 12.3$, 17.9, 19.5, 29.1, 45.9, 46.4, 47.6, 59.1, 83.2, 134.8, 159.6, 171.6 ppm; Anal. calcd for $C_{13}H_{19}N_2O_4$: C 58.41, H 7.16, N 10.48, found: C 58.65, H 6.88, N 10.18.

(±)-3-Phenyl-1-oxa-2,7-diaza-7,10-ethanospiro[4.5]dec-2-ene fumarate 5×0.5 $C_4H_4O_4$ (5a): Colorless prisms; mp: 191–192 °C (abs EtOH); ^1H NMR (300 MHz, D_2O): $\delta = 1.75$–1.95 (m, 3H), 2.18 (m, 2H), 3.15–3.33 (m, 4H), 3.35 (d, $J = 17.6$, 1H), 3.47 (d, $J = 14.3$, 1H), 3.53 (d, $J = 14.3$, 1H), 3.63 (d, $J = 17.6$, 1H), 6.48 (s, 1H), 7.31 (m, 3H), 7.50 ppm (m, 2H); ^{13}C NMR (75 MHz, D_2O): $\delta = 18.0$, 19.6, 29.4, 44.3, 46.2, 46.6, 59.1, 84.3, 126.8, 128.0, 129.1, 131.2, 134.7, 159.0, 171.6 ppm; Anal. calcd for $C_{17}H_{20}N_2O_3$: C 67.98, H 6.71, N 9.33, found: C 68.20, H 6.56, N 9.12.

(±)-3-Methoxy-1-oxa-2,7-diaza-7,10-ethanospiro[4.5]dec-2-ene fumarate 6×1.5 $C_4H_4O_4$ (6a): Colorless prisms; mp: 139–140 °C (2-propanol); ^1H NMR (300 MHz, D_2O): $\delta = 1.76$ (m, 2H), 1.93 (m, 1H), 2.14 (m, 1H), 2.30 (br s, 1H), 3.03 (d, $J = 16.9$, 1H), 3.07–3.32 (m, 4H), 3.19 (d, $J = 16.9$, 1H), 3.45 (d, $J = 14.7$, 1H), 3.49 (d, $J = 14.7$, 1H), 3.69 (s, 3H), 6.59 ppm (s, 3H); ^{13}C NMR (75 MHz, D_2O): $\delta = 17.6$, 19.4, 28.9, 41.3, 45.9, 46.5, 57.6, 58.7, 84.4, 134.5, 169.0, 170.5 ppm; Anal. calcd for $C_{16}H_{22}N_2O_8$: C 51.89, H 5.99, N 7.56, found: C 51.67, H 6.03, N 7.30.

(±)-3-Ethoxy-1-oxa-2,7-diaza-7,10-ethanospiro[4.5]dec-2-ene fumarate 7×0.75 $C_4H_4O_4$ (7a): Colorless prisms; mp: 167–168 °C (abs EtOH); ^1H NMR (300 MHz, D_2O): $\delta = 1.12$ (t, $J = 7.0$, 3H), 1.71 (m, 2H), 1.86 (m, 1H), 2.07 (m, 1H), 2.23 (br s, 1H), 2.97 (d, $J = 16.8$, 1H), 3.00–3.25 (m, 5H), 3.41 (m, 2H), 3.96 (q, $J = 7.0$, 2H), 6.48 ppm (s, 1.5H); ^{13}C NMR (75 MHz, D_2O): $\delta = 13.7$, 17.6, 19.4, 28.9, 41.6, 45.9, 46.4, 58.6, 67.2, 83.9, 134.7, 168.2, 171.3 ppm; Anal. calcd for $C_{14}H_{21}N_2O_5$: C 56.55, H 7.12, N 9.42, found: C 56.29, H 7.31, N 9.58.

(±)-3-*n*-Propoxy-1-oxa-2,7-diaza-7,10-ethanospiro[4.5]dec-2-ene fumarate 8×$C_4H_4O_4$ (8a): Colorless prisms; mp: 116–117 °C (EtOAc/CH_2Cl_2/abs EtOH); ^1H NMR (300 MHz, D_2O): $\delta = 0.76$ (t, $J = 7.3$, 3H), 1.56 (m, 2H), 1.74 (m, 2H), 1.91 (m, 1H), 2.12 (m, 1H), 2.26 (br s, 1H), 3.0 (dd, $J = 2.6$ and 16.8, 1H), 3.02–3.27 (m, 5H), 3.44 (br s, 2H), 3.91 (t, $J = 6.6$, 2H), 6.57 ppm (s, 2H); ^{13}C NMR (75 MHz, D_2O): $\delta = 9.7$, 17.6, 19.4, 21.7, 28.9, 41.5, 46.0, 46.5, 58.6, 72.8, 84.0, 134.5, 168.4, 170.5 ppm; Anal. calcd for $C_{16}H_{24}N_2O_6$: C 56.46, H 7.11, N 8.23, found: C 56.49, H 7.38, N 7.97.

(±)-3-Benzyloxy-1-oxa-2,7-diaza-7,10-ethanospiro[4.5]dec-2-ene fumarate 9×0.75 $C_4H_4O_4$ (9a): Colorless prisms; mp: 122–123 °C (abs EtOH); ^1H NMR (300 MHz, D_2O): $\delta = 1.68$ (m, 2H), 1.88 (m, 1H), 2.09 (m, 1H), 2.22 (br s, 1H), 2.99 (d, $J = 17.2$, 1H), 3.10 (m, 4H),

3.16 (d, $J=17.2$, 1H), 3.39 (d, $J=14.3$, 1H), 3.43 (d, $J=14.3$, 1H), 4.97 (s, 2H), 6.49 (s, 1.5H), 7.26 ppm (m, 5H); ^{13}C NMR (75 MHz, D_2O): $\delta=17.6$, 19.4, 28.9, 41.5, 45.9, 46.5, 58.5, 72.4, 84.2, 128.3, 128.9, 129.0, 134.7, 135.0, 167.8, 171.5 ppm; Anal. calcd for $C_{19}H_{23}N_2O_5$: C 63.50, H 6.45, N 7.79, found: C 63.77, H 6.22, N 7.54.

(±)-3-Propargyloxy-1-oxa-2,7-diaza-7,10-ethanospiro[4.5]dec-2-ene fumarate 10×0.5 $C_4H_4O_4$ (10a): Colorless prisms; mp: 193–196 °C (2-propanol/MeOH); ^{1}H NMR (300 MHz, D_2O): $\delta=1.71$ (m, 2H), 1.85 (m, 1H), 2.08 (m, 1H), 2.24 (m, 1H), 2.79 (t, $J=2.2$, 1H), 2.99 (d, $J=16.8$, 1H), 3.02–3.17 (m, 4H), 3.16 (d, $J=16.8$, 1H), 3.41 (m, 2H), 4.56 (d, $J=2.2$, 2H), 6.35 ppm (s, 1H); ^{13}C NMR (75 MHz, D_2O): $\delta=17.4$, 19.3, 28.9, 41.3, 45.9, 46.4, 57.9, 58.6, 77.1, 77.5, 84.6, 135.2, 167.2, 173.5 ppm; Anal. calcd for $C_{14}H_{18}N_2O_4$: C 60.42, H 6.52, N 10.07, found: C 60.11, H 6.85, N 10.38.

(±)-1-Oxa-2,7-diaza-7,10-ethanospiro[4.5]decan-3-one fumarate 11×0.75 $C_4H_4O_4$ (11a): Colorless prisms; mp: 172–173 °C (*n*-hexane/EtOAc/MeOH); ^{1}H NMR (300 MHz, D_2O): $\delta=1.76$ (m, 2H), 1.94 (m, 1H), 2.17 (m, 1H), 2.37 (br s, 1H), 2.87 (d, $J=16.7$, 1H), 2.95 (d, $J=16.7$, 1H), 3.08–3.30 (m, 4H), 3.42 (dd, $J=2.2$ and 14.3, 1H), 3.51 (dd, $J=2.2$ and 14.3, 1H), 6.47 ppm (s, 1.5H); ^{13}C NMR (75 MHz, D_2O): $\delta=17.4$, 18.9, 28.1, 41.9, 46.1, 46.5, 57.2, 80.5, 134.8, 166.7, 171.6 ppm; Anal. calcd for $C_{12}H_{17}N_2O_5$: C 53.52, H 6.36, N 10.40, found: C 53.23, H 6.58, N 10.72.

(±)-2-Methyl-1-oxa-2,7-diaza-7,10-ethanospiro[4.5]decan-3-one fumarate 12×0.5 $C_4H_4O_4$ (12a): Colorless prisms; mp: 162–163 °C (*n*-hexane/abs EtOH); ^{1}H NMR (300 MHz, D_2O): $\delta=1.77$ (m, 2H), 1.95 (m, 1H), 2.16 (m, 1H), 2.36 (br s, 1H), 2.84 (d, $J=16.8$, 1H), 2.89 (d, $J=16.8$, 1H), 3.03 (s, 3H), 3.08–3.32 (m, 4H), 3.40 (dd, $J=2.6$ and 14.3, 1H), 3.56 (dd, $J=2.6$ and 14.3, 1H), 6.54 ppm (s, 1H); ^{13}C NMR (75 MHz, D_2O): $\delta=17.4$, 19.0, 28.4, 31.6, 41.6, 46.0, 46.4, 57.7, 80.7, 134.8, 168.4, 171.5 ppm; Anal. calcd for $C_{12}H_{18}N_2O_4$: C 56.68, H 7.13, N 11.02, found: C 56.90, H 7.19, N 10.76.

General procedure for the preparation of iodomethylates: CH_3I (450 μL, 7.23 mmol) was added to a solution of the free base (0.5 mmol) in MeOH (3 mL). The solution was left overnight at RT, then the solvent was removed under reduced pressure, quantitatively affording the crude quaternary salt.

(±)-3-Ethoxycarbonyl-1-oxa-2,7-diaza-7,10-ethanospiro[4.5]dec-2-ene methyl iodide (1b): Light yellow prisms; mp: 162–163 °C (abs EtOH); ^{1}H NMR (300 MHz, D_2O): $\delta=1.23$ (t, $J=7.0$, 3H), 1.93 (m, 2H), 2.07 (m, 1H), 2.27 (m, 1H), 2.34 (br s, 1H), 2.97 (s, 3H), 3.31 (d, $J=18.4$, 1H), 3.33–3.48 (m, 4H), 3.50 (d, $J=18.4$, 1H), 3.73 (br s, 2H), 4.26 ppm (q, $J=7.0$, 2H); ^{13}C NMR (75 MHz, D_2O): $\delta=$ 13.5, 19.1, 20.6, 29.4, 42.6, 51.8, 56.3, 56.9, 63.5, 68.1, 88.0, 152.9, 161.2 ppm; Anal. calcd for $C_{13}H_{21}IN_2O_3$: C 41.07, H 5.57, N 7.37, found: C 41.38, H 5.22, N 7.10.

(±)-3-Hydroxymethyl-1-oxa-2,7-diaza-7,10-ethanospiro[4.5]dec-2-ene methyl iodide (2b): Light yellow prisms; mp: 155–170 °C, dec. (2-propanol/abs EtOH); ^{1}H NMR (300 MHz, CD_3OD): $\delta=2.01$ (m, 2H), 2.14 (m, 1H), 2.29 (m, 1H), 2.39 (m, 1H), 3.04 (s, 3H), 3.17 (d, $J=17.6$, 1H), 3.36 (dd, $J=17.6$, 1H), 3.42–3.55 (m, 4H), 3.71 (dd, $J=2.5$ and 13.5, 1H), 3.79 (dd, $J=2.5$ and 13.5, 1H), 4.30 ppm (s, 2H); ^{13}C NMR (75 MHz, D_2O): $\delta=19.3$, 20.8, 29.0, 44.2, 51.8, 56.2, 56.6, 56.8, 68.4, 84.5, 160.7 ppm; Anal. calcd for $C_{11}H_{19}IN_2O_2$: C 39.07, H 5.66, N 8.28, found: C 38.85, H 5.41, N 8.54.

(±)-3-Bromo-1-oxa-2,7-diaza-7,10-ethanospiro[4.5]dec-2-ene methyl iodide (3b): Colorless prisms; mp: 112–114 °C (MeOH); ^{1}H NMR (300 MHz, CD_3OD): $\delta=2.01$ (m, 2H), 2.13 (m, 1H), 2.37 (m, 2H), 3.05 (s, 3H), 3.34 (m, 2H), 3.40 (d, $J=18.0$, 1H), 3.51 (m, 2H), 3.60 (d, $J=18.0$, 1H), 3.78 (dd, $J=1.8$ and 14.3, 1H), 3.84 ppm (dd, $J=1.8$ and 14.3, 1H); ^{13}C NMR (75 MHz, [D_6]DMSO): $\delta=20.7$, 24.4, 32.4, 44.8, 51.4, 55.0, 55.5, 65.9, 68.2, 143.5 ppm; Anal. calcd for $C_{10}H_{16}BrIN_2O$: C 31.03, H 4.17, N 7.24, found: C 31.22, H 3.98, N 7.38.

(±)-3-Methyl-1-oxa-2,7-diaza-7,10-ethanospiro[4.5]dec-2-ene methyl iodide (4b): Colorless prisms; mp: 201–203 °C (2-propanol/MeOH); ^{1}H NMR (300 MHz, D_2O): $\delta=1.75$–1.85 (m, 2H), 1.81 (s, 3H), 1.93 (m, 1H), 2.14 (m, 2H), 2.85 (s, 3H), 2.95 (d, $J=17.9$, 1H), 3.17 (d, $J=17.9$, 1H), 3.15–3.38 (m, 4H), 3.52 ppm (br s, 2H); ^{13}C NMR (75 MHz, D_2O): $\delta=12.4$, 19.4, 20.9, 29.0, 47.6, 51.8, 56.2, 56.8, 68.6, 83.8, 159.5 ppm; Anal. calcd for $C_{11}H_{19}IN_2O$: C 41.01, H 5.94, N 8.69, found: C 41.11, H 5.75, N 8.87.

(±)-3-Methoxy-1-oxa-2,7-diaza-7,10-ethanospiro[4.5]dec-2-ene methyl iodide (6b): Colorless prisms; mp: 221–222 °C (MeOH); ^{1}H NMR (300 MHz, D_2O): $\delta=1.79$ (m, 2H), 1.95 (m, 1H), 2.15 (m, 1H), 2.29 (m, 1H), 2.85 (s, 3H), 2.99 (d, $J=17.0$, 1H), 3.15 (d, $J=$ 17.0, 1H), 3.14–3.37 (m, 4H) 3.56 (m, 2H), 3.65 ppm (s, 3H); ^{13}C NMR (75 MHz, D_2O): $\delta=19.1$, 20.8, 28.9, 41.3, 51.8, 56.3, 56.8, 57.7, 68.1, 84.9, 168.9 ppm; Anal. calcd for $C_{11}H_{19}IN_2O_2$: C 39.07, H 5.66, N 8.28, found: C 39.35, H 5.81, N 7.97.

(±)-3-Ethoxy-1-oxa-2,7-diaza-7,10-ethanospiro[4.5]dec-2-ene methyl iodide (7b): Colorless prisms; mp: 180–181 °C (abs EtOH); ^{1}H NMR (300 MHz, D_2O): $\delta=1.14$ (t, $J=7.0$, 3H), 1.79 (m, 2H), 1.95 (m, 1H), 2.15 (m, 1H), 2.28 (br s, 1H), 2.85 (s, 3H), 2.98 (d, $J=17.0$, 1H), 3.15 (d, $J=17.0$, 1H), 3.17–3.38 (m, 4H), 3.55 (m, 2H), 3.98 ppm (q, $J=7.0$, 2H); ^{13}C NMR (75 MHz, D_2O): $\delta=13.8$, 19.1, 20.8, 28.9, 41.6, 51.8, 56.3, 56.8, 67.3, 68.1, 84.5, 168.2 ppm; Anal. calcd for $C_{12}H_{21}IN_2O_2$: C 40.92, H 6.01, N 7.95, found: C 50.16, H 5.87, N 8.12.

(±)-3-Propoxy-1-oxa-2,7-diaza-7,10-ethanospiro[4.5]dec-2-ene methyl iodide (8b): Colorless prisms; mp: 134–135 °C (EtOAc/2-propanol); ^{1}H NMR (300 MHz, D_2O): $\delta=0.78$ (t, $J=7.3$, 3H), 1.57 (m, 2H), 1.83 (m, 2H), 1.99 (m, 1H), 2.18 (m, 1H), 2.32 (br s, 1H), 2.88 (s, 3H), 3.04 (d, $J=17.2$, 1H), 3.16–3.38 (m, 5H), 3.59 (m, 2H), 3.93 ppm (t, $J=6.6$, 2H); ^{13}C NMR (75 MHz, D_2O): $\delta=9.7$, 19.1, 20.9, 21.8, 28.9, 41.5, 51.8, 56.3, 56.8, 68.1, 72.9, 84.5, 168.3 ppm; Anal. calcd for $C_{13}H_{23}IN_2O_2$: C 42.63, H 6.33, N 7.65, found: C 42.90, H 6.12, N 7.38.

(±)-3-Benzyloxy-1-oxa-2,7-diaza-7,10-ethanospiro[4.5]dec-2-ene methyl iodide (9b): Yellow prisms; mp: 184–185.5 °C (abs EtOH); ^{1}H NMR (300 MHz, D_2O): $\delta=1.77$ (m, 2H), 1.94 (m, 1H), 2.14 (m, 1H), 2.27 (br s, 1H), 2.84 (s, 3H), 3.03 (d, $J=17.1$, 1H), 3.18 (d, $J=$ 17.1, 1H), 3.12–3.38 (m, 4H), 3.54 (m, 2H), 4.98 (s, 2H), 7.27 ppm (m, 5H); ^{13}C NMR (75 MHz, D_2O): $\delta=19.1$, 20.8, 28.9, 41.5, 51.8, 56.3, 56.8, 68.0, 72.5, 84.7, 128.4, 128.9, 129.1, 135.0, 167.7 ppm; Anal. calcd for $C_{17}H_{23}IN_2O_2$: C 49.29, H 5.60, N 6.76, found: C 49.57, H 5.87, N 6.58.

(±)-3-Propargyloxy-1-oxa-2,7-diaza-7,10-ethanospiro[4.5]dec-2-ene methyl iodide (10b): Colorless prisms; mp: 186–187 °C (2-propanol/MeOH); ^{1}H NMR (300 MHz, D_2O): $\delta=1.74$ (m, 2H), 1.92 (m, 1H), 2.12 (m, 1H), 2.26 (m, 1H), 2.78 (t, $J=2.2$, 1H), 2.81 (s, 3H), 2.99 (d, $J=17.2$, 1H), 3.12–3.37 (m, 5H), 3.54 (m, 2H), 4.56 ppm (d, $J=2.2$, 2H); ^{13}C NMR (75 MHz, D_2O): $\delta=18.9$, 20.7, 28.8, 41.3, 51.8, 56.2, 56.7, 58.0, 68.0, 84.6, 85.1, 167.0, 169.0 ppm; Anal. calcd for $C_{13}H_{19}IN_2O_2$: C 43.11, H 5.29, N 7.73, found: C 42.81, H 5.55, N 7.95.

(±)-2-Methyl-1-oxa-2,7-diaza-7,10-ethanospiro[4.5]decan-3-one methyl iodide (12b): Colorless prisms; mp: 181–182 °C (2-propanol); ^{1}H NMR (300 MHz, D_2O): $\delta=1.86$ (m, 2H), 2.03 (m, 1H), 2.22 (m, 1H), 2.42 (br s, 1H), 2.88 (d, $J=18.0$, 1H), 2.92 (s, 3H), 3.03 (d, $J=18.0$, 1H), 3.06 (s, 3H), 3.17–3.42 (m, 4H), 3.60 (dd, $J=2.3$ and

14.3, 1H), 3.69 ppm (dd, $J=2.3$ and 14.3, 1H); ^{13}C NMR (75 MHz, D_2O): $\delta=18.9$, 20.4, 28.4, 31.6, 41.5, 51.8, 56.3, 56.7, 67.1, 81.1, 168.3 ppm; Anal. calcd for $C_{11}H_{19}IN_2O_2$: C 39.07, H 5.66, N 8.28, found: C 39.28, H 5.75, N 8.09.

Preparation of (*R*)-(−)-6a and (*S*)-(+)-6a: A solution of (*R*,*R*)-(−)-*O*,*O*′-dibenzoyl-L-tartaric acid (4.57 g, 12.75 mmol) in abs EtOH (75 mL) was added to a solution of (±)-**6** (2.50 g, 12.75 mmol) in MeOH (75 mL). The solid which formed upon standing was filtered (filtrate A) and, after three slow crystallizations from MeOH, solid (−)-B, (mp 159–160 °C, dec.), was submitted to X-ray analysis (see below and Figure 2). $[\alpha]_D^{20}=-96.4$ ($c=0.70$; CH_3OH); ^{1}H NMR (300 MHz, [D$_6$]DMSO): $\delta=1.54$–1.82 (m, 3H), 1.98 (m, 1H), 2.13 (br s, 1H), 2.94–3.12 (m, 4H), 2.98 (d, $J=16.8$, 1H), 3.16 (d, $J=16.8$, 1H), 3.27 (dd, $J=1.9$ and 15.1, 1H), 3.34 (dd, $J=1.9$ and 15.1, 1H), 3.72 (s, 3H), 5.65 (s, 2H), 7.50 (m, 4H), 7.64 (m, 2H), 7.93 ppm (m, 4H); ^{13}C NMR (75 MHz, [D$_6$]DMSO): $\delta=18.5$, 20.4, 29.8, 41.4, 45.3, 45.7, 57.5, 59.1, 72.7, 84.5, 129.4, 129.9, 130.1, 134.2, 165.5, 167.5, 168.8 ppm; Anal. calcd for $C_{28}H_{30}N_2O_{10}$: C 60.64, H 5.45, N 5.05, found: C 60.51, H 5.67, N 4.98. Solid (−)-B was dissolved in 20% aqueous NaOH (50 mL), extracted with CH_2Cl_2 (3×50 mL), dried over anhyd Na_2SO_4, and concentrated in vacuo. The residue was dissolved in MeOH, and a solution of fumaric acid (1.5 equiv) in MeOH was added to the mixture. After stirring at RT for 12 h, the reaction mixture was concentrated under reduced pressure to afford the crude fumarate quantitatively.

(*R*)-(−)-6×1.5 $C_4H_4O_4$ [(*R*)-(−)-6a]: Colorless prisms; mp: 146.5–147.5 °C (2-propanol); $[\alpha]_D^{20}=-23.7$ ($c=0.68$; CH_3OH); Anal. calcd for $C_{16}H_{22}N_2O_8$: C 51.89, H 5.99, N 7.56, found: C 52.15, H 6.17, N 7.29; Chiral HPLC analysis, eluent: *n*-hexane:2-propanol, 4:1; flow rate = 0.8 mL min^{-1}; $\lambda=220$ nm; $t_R=7.80$ min; *ee* = 96.2%.

Filtrate A was converted into the free base by concentrating the solution and dissolving the residue in 20% aqueous NaOH. Extraction with CH_2Cl_2 (3×50 mL), followed by drying over Na_2SO_4 and concentration in vacuo, yielded a residue (740 mg) that was dissolved in MeOH (60 mL) and combined with a solution of (*S*,*S*)-(+)-*O*,*O*′-dibenzoyl-D-tartaric acid (1.35 g) in MeOH (60 mL). The resulting salt was crystallized twice from MeOH [solid (+)-B; mp: 159–160 °C, dec.]; $[\alpha]_D^{20}=+97.5$ ($c=0.70$; CH_3OH); ^{1}H NMR and ^{13}C NMR data matched those reported above for the enantiomer; Anal. calcd for $C_{28}H_{30}N_2O_{10}$: C 60.64, H 5.45, N 5.05, found: C 60.72, H 5.50, N 4.94; Solid (+)-B was treated with fumaric acid and crystallized as described above.

(*S*)-(+)-6×1.5 $C_4H_4O_4$ [(*S*)-(+)-6a]: Colorless prisms; mp: 146.5–147.5 °C (2-propanol); $[\alpha]_D^{20}=+23.1$ ($c=0.65$; CH_3OH); Anal. calcd for $C_{16}H_{22}N_2O_8$: C 51.89, H 5.99, N 7.56, found: C 52.09, H 5.72, N 7.73; Chiral HPLC analysis (see above), $t_R=6.94$ min; *ee* = 95.3%.

X-Ray crystallography

X-Ray crystallographic analysis of the salt from (*R*)-6 and (*R*,*R*)-(−)-*O*,*O*′-dibenzoyl-L-tartaric acid: Colorless single crystals were obtained from a solution in MeOH. Crystal data: $C_{10}H_{17}N_2O_2$; 0.5 ($C_{18}H_{14}O_8$); 0.5 ($C_{18}H_{12}O_8$), $M_r=554.55$, orthorhombic, space group $P2_12_12$ (No. 18), $a=22.9390(5)$ Å, $b=14.664(3)$ Å, $c=7.9210(16)$ Å, $V=2664.4(8)$ Å^3, $Z=4$, $\rho_{cald}=1.382$ Mg m^{-3}, $F(000)=1168$, μ(Mo Kα) = 0.106 mm^{-1}, $T=122.0$ (5) K, crystal dimensions = 0.38×0.36×0.09 mm.

Data collection and processing: Diffraction data were collected on an Enraf–Nonius KappaCCD diffractometer using graphite monochromated Mo Kα radiation ($\lambda=0.71073$ Å).[32,33] Reflections were measured within the range $-29\le h\le 29$, $-19\le k\le 19$, $-10\le l\le 10$, ($2.25^\circ<\theta<27.50^\circ$). Data were reduced using the program EvalCCD.[34] Absorption correction was applied using the program NUMABS ($T_{min}=0.964$; $T_{max}=0.992$).[35,36] A total of 60896 reflections were averaged according to the point group symmetry 222, resulting in 6138 unique reflections ($R_{int}=0.045$ on F_o^2).

Structure solution and refinement: The structure was solved by the direct method using the SHELXS97 program[37] and refined using the program SHELXL97.[38] Full matrix least-squares refinement was performed on F^2, minimizing $\Sigma w(F_o^2-F_c^2)^2$, with anisotropic displacement parameters for non-hydrogen atoms. The tartaric acid and the tartrate ion are situated on a two-fold axis. The two half moieties were located and refined. The positions of all hydrogen atoms were located on intermediate difference electron density maps, and hydrogen atoms in aliphatic CH, as well as NH and OH moieties, were included in the observed positions and refined with fixed isotropic displacement parameters ($U_{iso}=1.2\,U_{eq}$ for CH and NH, $U_{iso}=1.5\,U_{eq}$ for OH). The remaining hydrogen atoms were included in the calculated positions with fixed isotropic displacement parameters ($U_{iso}=1.2\,U_{eq}$ for CH (aromatic), CH_2, $U_{iso}=1.5\,U_{eq}$ for CH_3). The refinement (377 parameters, 6138 reflections) converged at $R_F=0.0288$, $wR_{F2}=0.0739$ for 5797 reflections with $F_o>4\sigma(F_o)$; $w=1/[\sigma^2(F_o^2)+(0.0460P)^2+0.4508P]$, where $P=(F_o^2+2F_c^2)/3$; $S=1.062$. In the final difference, Fourier map maximum and minimum electron densities were 0.213 and −0.200 e Å^{-3}, respectively. Absolute configuration could not be assigned based on structure determination [Flack parameter = −0.3(5)];[39] however, the (*R*)-configuration of the basic moiety (compound **6**) could be appropriate, given its stereochemistry relative to the known configuration of the (*R*,*R*)-*O*,*O*′-dibenzoyl-L-tartrate ion. A very short hydrogen bond was observed between tartaric acid (donor) and the tartrate ion (acceptor) [O–H···O^{-1}: O–H 1.04(2) Å, H···O^{-1} 1.44(2) Å, O···O^{-1}: 2.479(1) Å, O–H···O^{-1}: 173(2) Å]. Complex atomic scattering factors for neutral atoms were incorporated as in SHELXL97.[38,40] Crystallographic data for the (*R*,*R*)-*O*,*O*′-dibenzoyl-L-tartrate of (*R*)-**6** have been deposited in the Cambridge Crystallographic Data Centre (deposition number CCDC 761547). Copies of the data can be obtained, free of charge, upon application to the site: http://www.ccdc.cam.ac.uk/data_request/cif.

Receptor binding assays

Tissue preparation: Cortex tissues were dissected, immediately frozen on dry ice, and stored at −80 °C for later use. For each experiment, cortex tissues from two rats were homogenized in 10 mL of a buffer solution (50 mM Na_3PO_4, 1 M NaCl, 2 mM ethylenediaminetetraacetic acid (EDTA), 2 mM ethylene glycol tetraacetic acid (EGTA), and 2 mM phenylmethylsulfonyl fluoride, pH 7.4) using a potter homogenizer; the homogenates were then diluted and centrifuged at 60000 *g* for 1.5 h. Total membrane homogenization, dilution, and centrifugation procedures were performed twice, then the pellets were collected, rapidly rinsed with a buffer solution (50 mM Tris-HCl, 120 mM NaCl, 5 mM KCl, 1 mM $MgCl_2$, 2.5 mM $CaCl_2$, and 2 mM phenylmethylsulfonyl fluoride, pH 7), and resuspended in the same buffer containing a mixture of 20 μg mL^{-1} of each of the following protease inhibitors: leupeptin, bestatin, pepstatin A, and aprotinin.

[^{3}H]Epibatidine binding: (±)-[^{3}H]Epibatidine, with a specific activity of 56–60 Ci mmol^{-1}, was purchased from Perkin–Elmer (Boston, MA); the non radioactive α-bungarotoxin, nicotine, and epibatidine were purchased from Sigma–Aldrich (Italy). It was previously reported that [^{3}H]epibatidine also binds to α-bungarotoxin binding receptors with nanomolar affinity.[42] In order to prevent the bind-

ing of [^{3}H]epibatidine to α-bungarotoxin binding receptors, membrane homogenates were pre-incubated with 2 μM α-bungarotoxin and then with [^{3}H]epibatidine. Saturation experiments were performed by incubating aliquots of cortex membrane homogenates with 0.01–2.5 nM concentrations of (±)-[^{3}H]epibatidine overnight at 4 °C. Nonspecific binding was determined in parallel by incubation in the presence of 100 nM unlabeled epibatidine. After incubation, the samples were filtered through a GFC filter soaked in 0.5% polyethylenimine and washed with 15 mL of a buffer solution (10 mM Na_3PO_4, 50 mM NaCl, pH 7.4), and the filters were counted in a β-counter. (±)-[^{3}H]Epibatidine binding to the α3β4 subtype was determined as described above, using membranes obtained from SH-SY5Y neuroblastoma cells preincubated with 2 μM α-bungarotoxin.[43]

[^{125}I]α-Bungarotoxin binding: Saturation binding experiments were performed using aliquots of cortex membrane homogenates incubated overnight with 0.1–10 nM concentrations of [^{125}I]α-bungarotoxin (specific activity = 200–213 Ci mmol^{-1}, Amersham) at room temperature. Nonspecific binding was determined in parallel by incubation in the presence of 1 μM unlabeled α-bungarotoxin. After incubation, the samples were filtered as described above, and the bound radioactivity was directly counted in a γ-counter.-[^{125}I]α-Bungarotoxin binding to the human α7 receptors and muscle type α1β1γδ receptors was determined as described above using membrane obtained from IMR32 neuroblastoma cells in the case of α7 human subtype,[44] and membranes obtained from TE671 cell line in the case of α1β1γδ muscle receptors.

Affinity of derivatives 1a–12a, 3b, 4b, and 6b–10b for nAChRs: Inhibition of radioligand binding by epibatidine, nicotine, and the test compounds was measured by pre-incubating cortex homogenates with increasing doses (10 pM–10 mM) of the reference nicotinic agonists epibatidine or nicotine, or the drugs to be tested, for 30 min at room temperature. This was followed by overnight incubation with a final [^{3}H]epibatidine concentration of 0.075 nM (for the α4β2 subtype), 0.15 nM (for the α3β4 subtype), or 1 nM [^{125}I]α-bungarotoxin (for both α7 and α1β1γδ subtypes), at the same temperatures as those used for the saturation experiments. These ligand concentrations were used for the competition binding experiments, because they are within the range of the ligand K_D values for the two different classes of nAChRs. For each compound, experimental data obtained from three saturation and three competition binding experiments were analyzed by means of a non-linear least squares procedure, using the LIGAND program as described by Munson and Rodbard.[29] The binding parameters were calculated by simultaneously fitting three independent saturation experiments, and the K_i values were determined by fitting the data of three independent competition experiments. Errors in the K_D and K_i values of the simultaneous fits were calculated using the LIGAND software and were expressed as percentage coefficients of variation.

Electrophysiological recordings: Human α4β2 nAChRs were expressed by stable transfection in the human HEK 293 cell line,[31b] while the human α7 nAChRs were expressed by stable transfection in the rat anterior pituitary GH4C1 cell line.[31a] The human 5-HT_{3A} and 5-HT_{3B} cDNAs were kindly provided by Dr. E. F. Kirkness, Institute for Genomic Research (Rockville, MD, USA), and were used to transiently transfect GH4C1 cells, plated at a density of $5–10 \times 10^4$ per 35 mm Petri dish and grown in Ham's F10 nutrient mixture, with 10% fetal bovine serum and 1% penicillin and streptomycin. Transient transfection was achieved by adding 1 μg human 5-HT_3 subunit cDNA to each dish, along with 4 μL lipofectamine. All culture media were purchased from Invitrogen (San Giuliano Milanese, Italy). Whole-cell current recordings were performed 2–3 days after plating. Recordings and data analysis were carried out using borosilicate glass patch pipettes (3- to 6 MΩ tip resistance) connected to an Axopatch 200 A amplifier (Axon Instruments, Foster City, CA). Data were stored on a PC computer using the PCLAMP10 software (Molecular Devices). During the recording period, cells were bathed in the following solution: 140 mM NaCl, 2 mM $CaCl_2$, 2.8 mM KCl, 2 mM $MgCl_2$, 10 mM Hepes/NaOH, and 10 mM glucose; pH 7.3. The patch pipettes were filled with a solution containing: 140 mM CsCl, 2 mM MgATP, 10 mM Hepes/CsOH, and 5 mM BAPTA; pH 7.3. Whole-cell capacitance and patch series resistance (5–15 MΩ) were estimated from slow transient compensations. A series resistance compensation of 85–90% was obtained in all cases. The cells were voltage-clamped at a holding potential of −70 mV and continuously perfused with a gravity-driven system using independent external tubes for the control and agonist-containing solutions. These tubes were positioned 50–100 μm from the patched cell and connected to a fast exchanger system (RSC-160, BioLogic, France). Dose–response relationships were constructed by sequentially applying different concentrations of agonists and normalizing the resulting current amplitudes to the value obtained by applying 200 μM ACh or 5-HT to the same cell, as appropriate. For quantitative estimations of agonist actions, dose–response relationships were fitted to the following Equation (1):

$$I = I_{max}\{[C]^{nH}/(EC_{50}{}^{nH}+[C]^{nH})\} \quad (1)$$

where I is the current amplitude induced by the agonist at concentration $[C]$, I_{max} denotes the maximal response of the cell, nH is the Hill coefficient, and EC_{50} is the concentration for which a half maximum response is induced.

Molecular modeling

Ligands docked into the receptor binding clefts were built using Sybyl 8.0 (Tripos Inc., St. Louis, MO) and preliminarily minimized at the DFT/b3Lyp/6–31 g* level as implemented in Gaussian09.[45] The amino groups were considered in the ionized form to better simulate physiological conditions. Docking experiments of selected ligands in the binding site created by chains D and E of our published model[22b] of α7 nAChRs were performed using the program GOLD 4.0.[46] The receptor active site radius was set equal to 11 Å from the indole nitrogen of Trp 148, responsible for the primary ligand anchoring point. The side chain of Gln 116 was not restrained during the docking calculation. The goldscore fitness function and the distribution of torsion angles were chosen as indicators of the quality of the docking results. Van der Waals and hydrogen bonding radii were set at 4.0 and 3.0 Å, respectively, while genetic algorithm parameters were kept at default values. Next, CA by hierarchical-agglomerative script (ACIAP)[47] was applied to select a solution and, therefore, a statistically significant binding mode. The resulting complexes were further optimized geometrically by means of molecular mechanics methods (Tripos force field), implemented in Sybyl 8.0. Figures were generated with PyMOL software.[48]

Acknowledgements

This research project was financially supported by the following grants: FIRB RBNE03FH5Y (C.D.M.), PRIN 2005054943 and 20072BTSR2 (F.C., C.G., and M.D.A.), EC Neurocypres (C.G.), Fondazione Cariplo 2006/0779/109251 (C.G.), Compagnia San Paolo

*grant 2005–1964 (C.G.), and a grant from the Associazione Oasi Maria SS, Troina, Italy (F.C.). We are indebted to Prof. P. Ernsberger (Case Western Reserve University; Cleveland, OH), for affinity data for (±)-**6a** toward the human cloned muscarinic receptor subtypes. The technical assistance of Mr. F. Hansen (University of Copenhagen; Copenhagen, Denmark), for X-ray data collection is gratefully acknowledged.*

Keywords: electrophysiological assays · neuronal nicotinic acetylcholine receptors · X-ray crystallography · α7 agonists · Δ^2-isoxazoline derivatives

[1] a) H. A. Lester, M. I. Dibas, D. S. Dahan, J. F. Leite, D. A. Dougherty, *Trends Neurosci.* **2004**, *27*, 329–336; b) S. M. Sine, A. G. Engel, *Nature* **2006**, *440*, 448–455.

[2] a) E. Tribollet, D. Bertrand, A. Marguerat, M. Raggenbass, *Neuroscience* **2004**, *124*, 405–420; b) A. A. Jensen, B. Frølund, T. Liljefors, P. Krogsgaard-Larsen, *J. Med. Chem.* **2005**, *48*, 4705–4745; c) M. N. Romanelli, P. Gratteri, L. Guandalini, E. Martini, C. Bonaccini, F. Gualtieri, *ChemMedChem* **2007**, *2*, 746–767; d) E. X. Albuquerque, E. F. R. Pereira, M. Alkondon, S. W. Rogers, *Physiol. Rev.* **2009**, *89*, 73–120.

[3] a) A. Karlin, *Nat. Rev. Neurosci.* **2002**, *3*, 102–114; b) P. A. Arneric, M. Holladay, M. Williams, *Biochem. Pharmacol.* **2007**, *74*, 1092–1101.

[4] a) C. Gotti, F. Clementi, *Prog. Neurobiol.* **2004**, *74*, 363–396; b) C. Gotti, M. Zoli, F. Clementi, *Trends Pharmacol. Sci.* **2006**, *27*, 482–491.

[5] a) N. S. Millar, *Biochem. Soc. Trans.* **2003**, *31*, 869–874; b) N. Le Novère, P.-J. Corringer, J.-P. Changeaux, *J. Neurobiol.* **2002**, *53*, 447–456.

[6] a) P.-J. Corringer, J.-P. Changeaux, *Annu. Rev. Pharmacol. Toxicol.* **2000**, *40*, 431–458; b) C. Gotti, M. Moretti, A. Gaimarri, A. Zanardi, F. Clementi, M. Zoli, *Biochem. Pharmacol.* **2007**, *74*, 1102–1111.

[7] S. Fucile, *Cell Calcium* **2004**, *35*, 1–8.

[8] a) P. M. Lippiello, M. Bencherif, T. A. Hauser, K. G. Jordan, S. R. Letchworth, A. A. Mazurov, *Expert Opin. Drug Discovery* **2007**, *2*, 1185–1203; b) S. L. Cincotta, M. S. Yorek, T. M. Moschak, S. R. Lewis, J. S. Rodefer, *Curr. Opin. Investig. Drugs* **2008**, *9*, 47–56; c) A. Taly, P.-J. Corringer, D. Guedin, P. Lestage, J.-P. Changeux, *Nat. Rev. Drug Discovery* **2009**, *8*, 733–750.

[9] R. A. Glennon, *Prog. Med. Chem.* **2004**, *42*, 55–123.

[10] a) C. Chiamulera, G. Fumagalli, *Cent. Nerv. Syst. Agents Med. Chem.* **2007**, *7*, 269–288; b) N. A. Horenstein, F. M. Leonik, R. L. Papke, *Mol. Pharmacol.* **2008**, *74*, 1496–1511.

[11] a) Z. Guan, X. Zhang, K. Blennow, K.; A. Nordberg, *Neuroreport* **1999**, *10*, 1779–1782; A. Nordberg, *Neuroreport* **1999**, *10*, 1779–1782; b) K. Hashimoto, K. Koike, E. Shimizu, M. Iyo, *Curr. Med. Chem.: Cent. Nerv. Syst. Agents* **2005**, *5*, 171–184; c) A. Olincy, J. G. Harris, L. L. Johnson, V. Pender, S. Kongs, D. Allensworth, J. Ellis, G. O. Zerbe, S. Leonard, K. E. Stevens, J. O. Stevens, L. Martin, L. E. Adler, F. Soti, W. R. Kem, R. Freedman, *Arch. Gen. Psychiatry* **2006**, *63*, 630–638.

[12] a) K. R. Tietje, D. J. Anderson, R. S. Bitner, E. A. Blomme, P. J. Brackemeyer, C. A. Briggs, K. E. Browman, D. Bury, P. Curzon, K. U. Drescher, J. M. Frost, R. M. Fryer, G. B. Fox, J. H. Gronlien, M. Håkerud, E. J. Gubbins, S. Halm, R. Harris, R. J. Helfrich, K. L. Kohlhaas, D. Law, J. Malysz, K. C. Marsh, R. L. Martin, M. D. Meyer, A. L. Molesky, A. L. Nikkel, S. Otte, L. Pan, P. S. Puttfarcken, R. J. Radek, H. M. Robb, E. Spies, K. Thorin-Hagene, J. F. Waring, H. Ween, H. Xu, M. Gopalakrishnan, W. H. Bunnelle, *CNS Neurosci. Ther.* **2008**, *14*, 65–82; b) T. A. Hauser, A. Kucinski, K. G. Jordan, G. J. Gatto, S. R. Wersinger, R. A. Hesse, E. K. Stachowiak, M. K. Stachowiak, R. L. Papke, P. M. Lippiello, M. Bencherif, *Biochem. Pharmacol.* **2009**, *78*, 803–812.

[13] H. Wang, M. Yu, M. Ochani, C. A. Amella, M. Tanovich, S. Susarla, J. H. Li, H. Wang, H. Yang, L. Ulloa, Y. Al-Abed, C. J. Czura, K. J. Tracey, *Nature* **2003**, *421*, 384–388.

[14] a) M. Rosas-Ballina, R. S. Goldstein, M. Gallowitsch-Puerta, L. Yang, S. I. Valdés-Ferrer, N. B. Patel, S. Chavan, Y. Al-Abed, H. Yang, K. J. Tracey, *Mol. Med.* **2009**, *15*, 195–202; b) M. S. Gurun, R. Parker, J. C. Eisenach, M. Vincler, *Anesth. Analg.* **2009**, *108*, 1680–1687; c) Y. Xiong, X. Zhao, Q. Sun, R. Li, C. Li; J. Ye, *Pharmacol. Biochem. Behav.* **2010**, *95*, 192–197; J. Ye, *Pharmacol. Biochem. Behav.* **2010**, *95*, 192–197.

[15] a) R. Faghih, M. Gopalakrishnan, C. A. Briggs, *J. Med. Chem.* **2008**, *51*, 701–712; b) E. Luttmann, J. Ludwig, A. Höffle-Maas, M. Samochocki, A. Maelicke, G. Fels, *ChemMedChem* **2009**, *4*, 1874–1882; c) J. Dunlop, T. Lock, B. Jow, F. Sitzia, S. Grauer, F. Jow, A. Kramer, M. R. Bowlby, A. Randall, D. Kowal, A. Gilbert, T. A. Comery, J. LaRocque, V. Soloveva, J. Brown, R. Roncarati, *J. Pharmacol. Exp. Ther.* **2009**, *328*, 766–776.

[16] F. M. Leonik, R. L. Papke, N. A. Horenstein, *Bioorg. Med. Chem. Lett.* **2007**, *17*, 1520–1522.

[17] G. Mullen, J. Napier, M. Balestra, T. DeCory, G. Hale, J. Macor, R. Mack, J. Loch 3rd, E. Wu, A. Kover, P. Verhoest, A. Sampognaro, E. Phillips, Y. Zhu, R. Murray, R. Griffith, J. Blosser, D. Gurley, A. Machulskis, J. Zongrone, A. Rosen, J. Gordon, *J. Med. Chem.* **2000**, *43*, 4045–4050.

[18] a) A. L. Bodnar, L. A. Corte *s*Burgos, K. K. Cook, D. M. Dinh, V. E. Groppi, M. Hajós, N. R. Higdon, W. E. Hoffmann, R. S. Hurst, J. K. Myers, B. N. Rogers, T. M. Wall, M. L. Wolfe, E. Wong, *J. Med. Chem.* **2005**, 48, 905–908; b) M. Hajós, R. S. Hurts, W. E. Hoffmann, M. Krause, T. M. Wall, N. R. Higdon, V. E. Groppi, *J. Pharmacol. Exp. Ther.* **2005**, *312*, 1213–1222.

[19] D. Feuerbach, K. Lingenhoehl, H.-R. Olpe, A. Vassout, C. Gentsch, F. Chaperon, J. Nozulak, A. Enz, G. Bilbe, K. McAllister, D. Hoyer, *Neuropharmacology* **2009**, *56*, 254–263.

[20] B. Biton, O. E. Bergis, F. Galli, A. Nedelec, A. W. Lochead, S. Jegham, D. Godet, C. Lanneau, R. Santamaria, F. Chesney, J. Léonardon, P. Granger, M. W. Debono, G. A. Bohme, F. Sgard, F. Besnard, D. Graham, A. Coste, A. Oblin, O. Curet, X. Vigè, C. Voltz, L. Rouquier, J. Souilhac, V. Santucci, C. Gueudet, D. Françon, R. Steinberg, G. Griebel, F. Oury-Donat, P. George, P. Avenet, B. Scatton, *Neuropsychopharmacology* **2007**, *32*, 1–16.

[21] B. A. Acker, E. J. Jacobsen, B. N. Rogers, D. G. Wishka, S. C. Reitz, D. W. Piotrowski, J. K. Myers, M. L. Wolfe, V. E. Groppi, B. A. Thornburgh, P. M. Tinholt, R. R. Walters, B. A. Olson, L. Fitzgerald, B. A. Staton, T. J. Raub, M. Krause, K. S. Li, W. E. Hoffmann, M. Hajós, R. S. Hurst, D. P. Walker, *Bioorg. Med. Chem. Lett.* **2008**, *18*, 3611–3615.

[22] a) L. Rizzi, C. Dallanoce, C. Matera, P. Magrone, L. Pucci, C. Gotti, F. Clementi, M. De Amici, *Bioorg. Med. Chem. Lett.* **2008**, *18*, 4651–4654; b) G. Grazioso, A. Cavalli, M. De Amici, M. Recanatini, C. De Micheli, *J. Comput. Chem.* **2008**, *29*, 2593–2603; c) G. Grazioso, D. Y. Pomè, C. Matera, F. Frigerio, L. Pucci, C. Gotti, C. Dallanoce, M. De Amici, *Bioorg. Med. Chem. Lett.* **2009**, *19*, 6353–6357; d) C. De Micheli, M. De Amici, C. Dallanoce, F. Clementi, C. Gotti, PCT Int. Appl. WO 2008000469, **2008**, *47* pp; e) J. Sgrignani, C. Bonaccini, G. Grazioso, M. Chioccioli, A. Cavalli, P. Gratteri, *J. Comput. Chem.* **2009**, *30*, 2443–2454.

[23] a) P. Conti, M. De Amici, G. Grazioso, G. Roda, F. F. Barberis Negra, B. Nielsen, T. Bryan Stensbøl, U. Madsen, H. Bräuner-Osborne, K. Frydenvang, G. De Sarro, L. Toma, C. De Micheli, *J. Med. Chem.* **2004**, *47*, 6740–6748; b) C. Dallanoce, G. Meroni, M. De Amici, C. Hoffmann, K.-N. Klotz, C. De Micheli, *Bioorg. Med. Chem.* **2006**, *14*, 4393–4401; c) C. Dallanoce, P. Magrone, C. Matera, L. Lo Presti, M. De Amici, L. Riganti, F. Clementi, C. Gotti, C. De Micheli, *Eur. J. Med. Chem.* **2010**, *45*, 5594–5601.

[24] C. K. Y. Lee, C. J. Easton, G. P. Savage, G. W. Simpson, *ARKIVOC* **2006** (iii), 175–183.

[25] A. P. Kozikowski, M. Adamczyk, *J. Org. Chem.* **1983**, *48*, 366–372.

[26] P. L. Slotter, M. D. Friedman, G. O. Dorsey, R. W. Shiely, R. F. Williams, D. E. Minter, *Heterocycles* **1987**, *25*, 251–258.

[27] a) D. M. Vyas, Y. Chiang, T. W. Doyle, *Tetrahedron Lett.* **1984**, *25*, 487–490; b) C. Dallanoce, P. Magrone, P. Bazza, G. Grazioso, L. Rizzi, L. Riganti, C. Gotti, F. Clementi, K. Frydenvang, M. De Amici, *Chem. Biodiversity* **2009**, *6*, 244–259; c) G. A. Lee, *Synthesis* **1982**, 508–509.

[28] M. De Amici, C. De Micheli, V. Misani, *Tetrahedron* **1990**, *46*, 1975–1986.

[29] P. J. Munson, D. Rodbard, *Anal. Biochem.* **1980**, *107*, 220–239.

[30] D. G. Wishka, D. P. Walker, K. M. Yates, S. C. Reitz, S. Jia, J. K. Myers, K. L. Olson, E. J. Jacobsen, M. L. Wolfe, V. E. Groppi, A. J. Hanchar, B. A. Thornburgh, L. A. Corte *s*Burgos, E. H. F. Wong, B. A. Staton, T. J. Raub, N. R. Higdon, T. M. Wall, R. S. Hurst, R. R. Walters, W. E. Hoffmann, M. Hajos, S. Franklin, G. Carey, L. H. Gold, K. K. Cook, S. B. Sands, S. X. Zhao, J. R. Soglia, A. S. Kalgutkar, S. P. Arneric, B. N. Rogers, *J. Med. Chem.* **2006**, 49, 4425–4436.

[31] a) S. Fucile, M. Renzi, P. Lax, F. Eusebi, *Cell Calcium* **2003**, *34*, 205–209; b) E. Palma, F. Trettel, S. Fucile, M. Renzi, R. Miledi, F. Eusebi, *Proc. Natl. Acad. Sci. USA* **2003**, *100*, 2896–2900.

[32] COLLECT. B. V. Nonius Delft, The Netherlands, 1999.
[33] A. J. M. Duisenberg, *J. Appl. Crystallogr.* **1992**, *25*, 92.
[34] A. J. M. Duisenberg, EvalCCD, PhD Thesis, University of Utrecht, The Netherlands, 1998.
[35] P. Coppens in *Crystallographic Computing*, (Eds.: F. R. Ahmed, S. R. Hall, C. P. Huber), Munksgaard, Copenhagen, **1970**, pp. 255 – 270.
[36] S. Mackay, C. J. Gilmore, C. Edwards, N. Stewart, K. Shankland, Bruker Nonius, The Netherlands, Mac-Science, Japan, The University of Glasgow, **1999**. Procedure NUMABS.
[37] a) G. M. Sheldrick, SHELXS97, *Program for the Solution of Crystal Structures*, University of Göttingen, Göttingen, Germany, **1997**; b) G. M. Sheldrick, *Acta Crystallogr. Sect. A* **1990**, *46*, 467 – 473.
[38] G. M. Sheldrick, SHELXL97, *Program for Crystal Structure Refinement*, University of Göttingen, Göttingen, Germany, **1997**.
[39] H. D. Flack, *Acta Crystallogr. Sect. A* **1983**, *39*, 876 – 881.
[40] *International Tables for Crystallography*, (Ed.: A. J. C. Wilson), Kluwer Academic Publishers, Dordrecht, The Netherlands, **1995**; Vol. C, Tables 4.2.6.8 and 6.1.1.4.
[41] L. J. Farrugia, *J. Appl. Crystallogr.* **1997**, *30*, 565.
[42] V. Gerzanich, X. Peng, F. Wang, G. Wells, R. Anand, S. Fletcher, J. Lindstrom, *Mol. Pharmacol.* **1995**, *48*, 774 – 782.
[43] B. Balestra, M. Moretti, R. Longhi, R. Mantegazza, F. Clementi, C. Gotti, *J. Neuroimmunol.* **2000**, *102*, 89 – 97.
[44] C. Gotti, L. Briscini, C. Verderio, M. Oortgisien, B. Balestra, F. Clementi, *Eur. J. Neurosci.* **1995**, *7*, 2083 – 2092.
[45] Gaussian 09, Revision A.02, M. J. Frisch, G. W. Trucks, H. B. Schlegel, G. E. Scuseria, M. A. Robb, J. R. Cheeseman, G. Scalmani, V. Barone, B. Mennucci, G. A. Petersson, H. Nakatsuji, M. Caricato, X. Li, H. P. Hratchian, A. F. Izmaylov, J. Bloino, G. Zheng, J. L. Sonnenberg, M. Hada, M. Ehara, K. Toyota, R. Fukuda, J. Hasegawa, M. Ishida, T. Nakajima, Y. Honda, O. Kitao, H. Nakai, T. Vreven, J. A. Montgomery, Jr., J. E. Peralta, F. Ogliaro, M. Bearpark, J. J. Heyd, E. Brothers, K. N. Kudin, V. N. Staroverov, R. Kobayashi, J. Normand, K. Raghavachari, A. Rendell, J. C. Burant, S. S. Iyengar, J. Tomasi, M. Cossi, N. Rega, J. M. Millam, M. Klene, J. E. Knox, J. B. Cross, V. Bakken, C. Adamo, J. Jaramillo, R. Gomperts, R. E. Stratmann, O. Yazyev, A. J. Austin, R. Cammi, C. Pomelli, J. W. Ochterski, R. L. Martin, K. Morokuma, V. G. Zakrzewski, G. A. Voth, P. Salvador, J. J. Dannenberg, S. Dapprich, A. D. Daniels, Ö. Farkas, J. B. Foresman, J. V. Ortiz, J. Cioslowski, and D. J. Fox, Gaussian, Inc., Wallingford CT, 2009.
[46] GOLD v. 4.0, Cambridge Crystallographic Data Centre: Cambridge, UK.
[47] a) G. Bottegoni, A. Cavalli, M. Recanatini, *J. Chem. Inf. Model.* **2006**, *46*, 852 – 862; b) G. Bottegoni, W. Rocchia, M. Recanatini, A. Cavalli, *Bioinformatics* **2006**, *22*, e58-e65.
[48] W. L. DeLano, The PyMOL Molecular Graphics System (**2002**), DeLano Scientific, Palo Alto, CA, USA. [http://www.pymol.org].

Received: November 26, 2010
Revised: January 13, 2011
Published online on March 1, 2011

